Institut für Radiochemie

Production and chemical processing of ^{177}Lu for nuclear medicine at the Munich research reactor FRM-II

Dissertation
of
Zuzana Dvořáková

Technische Universität München

Institut für Radiochemie der Technischen Universität München

Production and chemical processing of ^{177}Lu for nuclear medicine at the Munich research reactor FRM-II

Zuzana Dvořáková

Vollständiger Abdruck der von der Fakultät für Chemie
der Technischen Universität München zur Erlangung des akademischen Grades eines

Doktors der Naturwissenschaften (Dr. rer. nat.)

genehmigten Dissertation.

Vorsitzender: Univ.-Prof. Dr. Dr. h. c. B. Rieger
Prüfer der Dissertation:

1. Univ.-Prof. Dr. A. Türler
2. Univ.-Prof. Dr. K. Köhler

Die Dissertation wurde am 13.8.2007 bei der Technischen Universität München eingereicht und durch die Fakultät für Chemie am 20.9.2007 angenommen.

Abstract

The main goal of the present dissertation was to investigate the feasibility of producing the radionuclide ^{177}Lu at the Munich research reactor FRM-II. Lutetium-177 represents an ideal therapeutic radioisotope with suitable chemical properties and nuclear decay characteristics. Radiopharmaceuticals containing ^{177}Lu are currently under development and tested for the treatment of various cancers in dozens of clinical trials around the world.

The radionuclide ^{177}Lu can be produced either directly by the $^{176}\mathrm{Lu}(n,\gamma)^{177}\mathrm{Lu}$ reaction or indirectly by the $^{176}\mathrm{Yb}(n,\gamma)^{177}\mathrm{Yb} \xrightarrow{\beta^-} {}^{177}\mathrm{Lu}$ reaction. The irradiation yield of ^{177}Lu in both production routes was experimentally determined and compared with theoretical calculations. A reliable method for the calculation of the ^{177}Lu yield, based on the Westcott convention, was established, which is more accurate than the methods published in the literature. The neutron flux parameters of FRM-II were determined, a prerequisite for a succesful application of the Westcott convention. The 160.5-day isomer $^{177\mathrm{m}}$Lu was experimentally confirmed to be the only relevant long-lived radionuclidic impurity found in ^{177}Lu produced by activation of enriched ^{176}Lu targets. A procedure to recover the produced ^{177}Lu from the direct production reaction in a closed system excluding the introduction of impurities was developed. The system will allow the integration of remote control or simple robotics, which will be necessary for handling highly active samples.

Acknowledgements

This dissertation is the result of research conducted at the Institut für Radiochemie der Technischen Universität München from May 2004 till August 2007 under the supervision of Prof. Dr. Andreas Türler.

First of all, I would like to thank my "Doktorvater", Prof. Dr. Andreas Türler, for giving me the opportunity to work on such an interesting topic. I thank him for the continuous support in all areas, for the possibility to present my work at several conferences, and for a careful reading and correction of this work. I am grateful for his trust in my abilities and for his unreserved and friendly attitude.

I would like to thank Dr. Jörg Brockmann, who was my mentor at the very beginning of my Ph.D.. He provided me with the initial orientation at RCM, introduced me to the branch of nuclear medicine, and learned me the basics of HPLC. In spite of being non-smoker myself, I enjoyed our talks during the cigarette breaks.

Further, I would like to thank Dr. Xilei Lin for learning me the basics of neutron activation analysis and for his kind guidance on the field of γ-spectrometry. He was always ready to help and pass some of his experience in irradiation techniques to me.

I would like to thank the staff at the Munich reactor FRM-II for conducting the irradiations of my samples. In particular, I would like to thank Dr. Heiko Gerstenberg for executing my irradiation requests promptly, and to Dr. X. Li, M. Oberndorfer, and G. Langenstück for their help.

I thank my colleagues Christine Kardinal, Sonja Buchheit, and Dr. Dirk Dautzenberg for carrying out the ICP-OES and ICP-MS analysis of my samples, Frank Klein for performing the SEM/EDX analysis, Wolfgang Stöwer for the irradiation of my

samples with the ^{60}Co γ-source, and Siegfried Firley for producing and sealing the quartz ampoules. I appreciate the help of Christoph Barkhausen by performing the last experiments. I am indebted to Dr. Eva Kabai and Dr. Josue Moreno for reading this work and for their valuable comments. I thank Guy Birebent for the help with the radioactive waste disposal. I thank Dr. Richard Henkelmann and Irmgard Kaul for their help and advices in all the administrative tasks. I thank the colleagues from the mechanical workshop of the institute for their help in whatever was needed.

I would like to thank all the colleagues and friends from the institute for the warm acceptance in the institute's team, for their everyday support, and for the interesting talks we had. I will always remember the excellent working group of the institute that I could be part of.

Special thanks go to my parents for supporting me throughout all my studies and for their confidence and toleration. Finally, I would like to thank my husband for his love, support, immense patience, and help with IT problems. Without him standing at my side, this work could hardly be finished.

Thank you all!

Contents

Abbreviations

c.a.	carrier-added
cf.	compare
CRL	Chalk River Laboratories
DOTATATE	[DOTA^0,Tyr^3]octreotate
DOTATOC	[DOTA^0,Tyr^3]octreotide
EDTA	ethylenediaminetetraacetic acid
e.g.	exempli gratia = for example
EOB	end of bombardment
FRM-II	Forschungsneutronenquelle Heinz Maier-Leibnitz in Garching bei München
GRP	gastrin releasing peptide
GSI	Gesellschaft für Schwerionenforschung in Darmstadt
HDEHP	di(2-ethylhexyl) orthophosphoric acid
HFIR	High Flux Isotope Reactor operated by ORNL
i.e.	id est = that is
HPLC	high performance liquid chromatography
ICP-MS	inductively coupled plasma - mass spectroscopy
ICP-OES	inductively coupled plasma - optical emission spectroscopy
IUPAC	International Union of Pure and Applied Chemistry
KBA 1-1	Kapsel-Bestrahlungsanlage 1-1
LET	linear energy transfer
LSC	liquid scintillation counting
MURR	University of Missouri Research Reactor Center
n.c.a.	no-carrier-added
NPP	nuclear power plant
NRU	National Research Universal reactor

ORNL	Oak Ridge National Laboratory
RCM	Institut für Radiochemie
SSC RIAR	State Scientific Center of Russian Federation Research Institute of Atomic Reactors
TRT	targeted radiotherapy
TUM	Technische Universität München

Chapter 1

Motivation

Radionuclides play an important role in our lives, finding numerous applications in industry, agriculture, and research, as well as in medicine. Widespread production of radionuclides for nuclear medicine began in the early 1950s. Currently, radiopharmaceuticals are used mainly for diagnostic imaging studies (^{99m}Tc, [1]), however, therapeutic applications are showing a substantial growth in the last few years. Traditional external radiation therapy is carried out using γ or X-ray sources. Other types of external therapies include e.g. boron neutron capture therapy (treatment of glioblastoma and malignant melanoma) [2], proton beam therapy (eye tumors) [3], and ^{12}C beam therapy (deep-seated localized tumors) [4]. Another possibility is internal radiotherapy, which is performed by administering or planting a small radiation source in the target area. One of the most successful kinds of cancer treatment is the treatment of thyroid cancer with ^{131}I [5]. Many therapeutic procedures are palliative, aimed at relieving bone pain from skeletal metastases (^{89}Sr, ^{186}Re, ^{153}Sm) [6]. The pure β^- emitter ^{90}Y is used for the treatment of non-Hodgkin's lymphoma [7] and arthritis [8, 9].

The demand for therapeutic radioisotopes is still growing and the only reason that could hinder their application would be insufficient supply. Because most therapeutic radionuclides are neutron rich and decay by β^- emission, they are produced in nuclear reactors. However, to produce these isotopes, a high-purity thermal neutron spectrum and a special reactor design is required, which means that production is mostly carried out at dedicated nuclear reactors or at research reactors. In 2004,

the new moderate-flux research reactor FRM-II, fulfilling the requirements for radioisotope production, started its operation in Garching. Hereby, a new research field has been opened at the Institute for Radiochemistry (RCM), which is settled on the same premises as the reactor and has direct connection to it through a pneumatic rabbit system. The production of therapeutic radionuclides and their chemical processing represents a very vivid research area. The first radioisotope selected, to be investigated at RCM, was ^{177}Lu, an ideal therapeutic radioisotope with suitable nuclear decay characteristics and the possibility to transfer the gained experience to other lanthanides. Radiopharmaceuticals containing ^{177}Lu are currently under development and tested for the treatment of various cancers in dozens of clinical trials around the world. At present, no producer of high specific activity ^{177}Lu exists in Europe and clinics are dependent on the supplies from the U.S.A., Canada, and Russia. Unfortunately, the quality of ^{177}Lu preparations decreases with the time needed for delivery and the price increases. The production of ^{177}Lu at FRM-II followed by its chemical processing at RCM would be very beneficial as a fast delivery to the whole of Europe can be quaranteed thanks to the close-by international airport.

The scope of the present dissertation was the production of carrier-added and no-carrier-added ^{177}Lu via direct (^{176}Lu (n,γ) ^{177}Lu) and indirect (^{176}Yb$(n,\gamma)^{177}$Yb $\xrightarrow{\beta^-}$ ^{177}Lu) production ways. The particular goals included the determination of the ^{177}Lu production yields in both reactions, the choice of a suitable irradiation position, the optimization of irradiation and decay times, the determination of the radionuclidic purity of the product, the development of target handling procedures, and especially the development of an effective method for the separation of produced ^{177}Lu from ytterbium target material in the case of the indirect production route.

Chapter 2

Introduction

In this chapter, the principles and requirements of targeted radiotherapy are discussed. Further, therapeutic radionuclides including ^{177}Lu are introduced. The ^{177}Lu production routes are described, together with a detailed overview and discussion of Lu/Yb separation methods.

2.1 Targeted radiotherapy

Radionuclide therapy employing open sources of radiotherapeutic agents is rapidly emerging as an important part of nuclear medicine, primary due to the development of a diversity of sophisticated molecular carriers (radioactive microspheres, labeled small molecules, isotopically-tagged monoclonal antibodies or antibody fragments, and labeled polypeptide receptor agents). The targeted radiotherapy (TRT) with its ability to deliver the radiation dose preferably to cancer cells (even when their location in the body is unknown) is a quickly developing modality of cancer treatment and treatment of other pathological conditions such as rheumatoid arthritis. Lutetium-177, whose production was studied in the framework of this dissertation, is a very promising radionuclide for use in TRT.

2.1.1 Principle and requirements

A typical radiopharmaceutical used in TRT consists of two components - the radionuclide which is responsible for the therapeutic effect and a biolocalization agent such as a peptide or an antibody which is responsible for the delivery of the attached radionuclide to malignant cells. A sketch of the TRT principle is shown in Fig. 2.1.

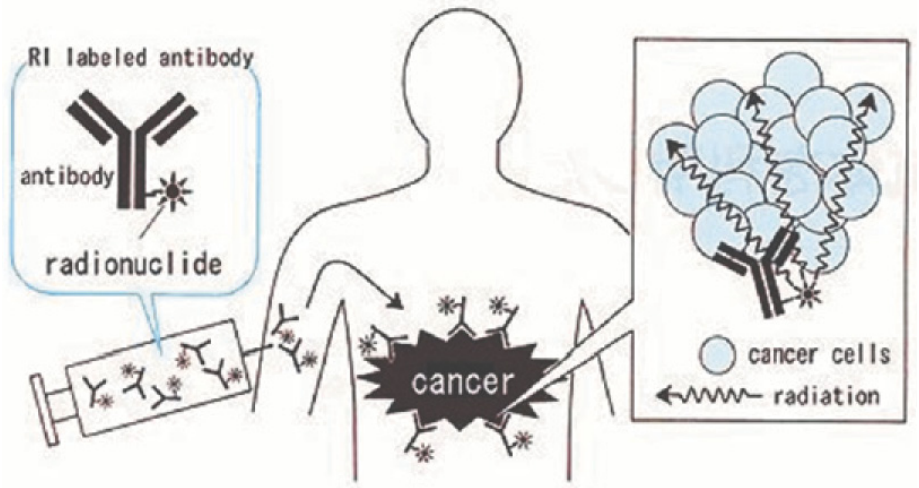

Figure 2.1: The simplified principle of targeted radiotherapy.

A radionuclide has to meet certain requirements with respect to its decay characteristics, biochemical reactivity and availability, to be a promising candidate for TRT [5, 10, 11]. The radionuclide should emit corpuscular radiation with a suitable linear energy transfer value and range in the tissue. It should also emit low abundant imageable γ rays for imaging the uptake and biodistribution of the therapeutic agent and for subsequent dosimetry. The half-life of the radionuclide should be matched well with the in vivo biolocalization and clearance properties of the radiolabeled drug. Further, it should be long enough to permit the synthesis of radiopharmaceutical, the quality control, and eventual distribution to more distant customers. The daughter isotope should be short-lived or stable. Important indicators are also the availability of the radionuclide with high specific activity and radionuclidic purity.

2.1.2 Specific activity and purity

The specific activity, A_s, for a given radionuclide is defined as its activity divided by the total mass of all its radioactive and stable isotopes. The units are Bq/mol or Bq/g, but the older units Ci/mol and Ci/g are still widely used. The value of the specific activity depends primarily on the method of production. Simple neutron capture reactions (n, γ) generally give low specific activity since the radionuclide cannot be chemically separated from the target of the same element. The higher the thermal neutron flux, cross section of the reaction, and isotopic enrichment of the target, the higher the specific activity that can be reached. Radionuclide preparations produced in such a manner are called carrier-added (*c.a.*). No-carrier-added (*n.c.a.*) preparations of a given radionuclide are such preparations, where special attention has been paid to procedures, equipment and materials in order to minimize the introduction of isotopes (both stable and radioactive) of the element in question into the system [12]. Accelerator-based proton-, deuteron-, or alpha-induced reactions are intrinsically *n.c.a.* methods that do allow chemical separation of the product from the target material. This can be also achieved at reactors by neutron capture reactions leading to a product which decays by β^- to the desired final product, or by fast neutron reactions, such as (n, p).

Depending on the nature of the molecule that will be labeled, high specific activity may be required. One example of the importance of high specific activity is the radiolabeling of tumor-specific antibodies or peptides for both diagnostic and therapeutic applications where only very small amounts of the radiolabeled antibodies are administered to ensure maximum uptake at the limited tumor cell surface antigen sites. Another case is the use of receptor-mediated radiopharmaceuticals that are potentially very important for the clinical evaluation of neurological diseases. Since the population of neurotransmitter sites is very limited, high specific activity agents are required to evaluate site-specific uptake without saturating these binding sites with stable isotopes [13].

A high degree of radionuclidic and chemical purity is required for therapeutic radionuclides. Impurities of other chemical elements can compete with the radioisotope for binding sites or ligands during the labeling of a radiopharmaceutical, decreasing the efficiency of this process. The chemical purity has to also satisfy the requirements for in vivo application. Eventual radionuclidic impurities constitute an unnecessary

burden for a patient and when long-lived complicate the waste disposal.

2.1.3 Therapeutic radionuclides

Radionuclides emitting particles represent a perfect tool for depositing high energy amounts in a small volume and therefore are especially suitable for therapy of various cancers. Radionuclides that decay by β particle emission, α particle emission, and Auger electron emission have been used in unsealed source radiotherapeutic agent development [5, 14]. Each type of these particles has different effective range and linear energy transfer (LET) properties. The type of particle emission that is applicable for the treatment depends on the size of the tumor, intra-tumor distribution, pharmacokinetics of the tracer, and other factors. Some radionuclides used in TRT are listed in Tab. 2.1.

Beta emitters were first to be utilized in patients for radionuclide therapy and still remain the type of radionuclides used most frequently. The β^- particles are emitted from the nucleus with energies ranging from almost zero up to a maximum value. They have typical ranges in tissue of 1–10 mm, and thus provide homogeneous tumor dosage even though their deposition is heterogeneous in target tissues. Of particular interest are radiolanthanides (listed in the second part of Tab. 2.1), which can be conveniently produced with high yields at research reactors. As they have similar chemical characteristics, their production and use in therapeutic radiopharmaceuticals can be based on similar principles providing a range of half-lives, LET values, and tissue ranges to choose from.

Alpha emitting radionuclides are very attractive for tumor therapy because of their high LET and thus high cytotoxicity. They were proposed to be especially useful for treatment of single cancer cells in circulation and small cancer cell clusters. However, most α emitters are heavy elements that decay to radioactive, long-lived daughter products, so that only a small number of α emitting radionuclides can be useful for medical application.

Table 2.1: Selected radionuclides for targeted radiotherapy [1, 15]. $\overline{E}_\beta$ is the average β energy, E_α is the energy of α particles, E_γ is the energy of photons. Radiolanthanides are given in the second half of the table.

Radionuclide	Half-life, days	Decay mode	$\overline{E}_\beta$, keV E_α, MeV	E_γ, keV (abundance)
^{131}I	8.0	β^-, γ	182	364(100%)
^{90}Y	2.7	β^-	934	-
^{67}Cu	2.6	β^-, γ	141	93(16%), 185(49%)
^{188}Re	0.7	β^-, γ	763	155(16%)
^{213}Bi	0.03	α, γ	5.84, 8.38	440(26%)
^{225}Ac	10	α	5.75, 6.36, 7.07, 8.38	-
^{111}In	2.8	Auger e^-, γ	32	171(91%), 245(94%)
^{142}Pr	0.8	β^-	809	-
^{143}Pr	13.6	β^-	215	-
^{149}Pm	2.2	β^- , γ	364	286(3%)
^{153}Sm	1.9	β^- , γ	224	103(29%)
^{159}Gd	0.8	β^- , γ	303	364(12%)
^{161}Tb	6.9	β^- , γ	154	75(10%)
^{166}Ho	1.1	β^- , γ	666	81(7%)
^{169}Eb	9.4	β^-	100	-
^{175}Yb	4.2	β^- , γ	113	396(13%)
^{177}Lu	6.7	β^- , γ	134	208(10%), 113(6%)

2.2 Radionuclide ^{177}Lu

2.2.1 Properties and comparison with other therapeutic radionuclides

In recent years, ^{177}Lu has emerged as a promising short-range β emitter for targeted radiotherapy. It can be employed as an alternative to ^{131}I or a complement to ^{90}Y, which are two routinely used therapeutic radionuclides. Properties of these radionuclides, together with ^{177}Lu are listed in Table 2.1. Due to low energetic beta radiation,

^{177}Lu is ideal for treating micro-metastatic diseases where ^{90}Y would unnecessarily expose the normal tissue surrounding the tumor. Since ^{90}Y emits no γ rays, ^{111}In is usually paired with ^{90}Y as a surrogate radionuclide to obtain information about the patient specific distribution and dosimetry. However, questions remain about the similarity of indium and yttrium behavior in patients [16]. There is no need to use a surrogate with ^{177}Lu because it itself emits well-imageable γ radiation. Iodine-131 emits γ rays, which are not well suited for imaging. Further, high energy γ radiation complicates the radiotherapy procedure by increasing the radiation dose to the patient and to the health care personnel and by the necessity to isolate patients in shielded rooms until the body radioactivity has decayed. Such measures are not needed if ^{177}Lu is used. The ^{177}Lu half-life of 6.65 days allows the employment of more sophisticated procedures to synthesize and purify radiopharmaceuticals and further enables its transport to more distant customers.

Several radiopharmaceuticals containing ^{177}Lu are under investigation and in clinical trials. The most studied are DOTA-conjugated peptides, such as [DOTA^0,Tyr^3] octreotide (DOTATOC) and [DOTA^0,Tyr^3]octreotate (DOTATATE) labeled with ^{177}Lu, used for peptide receptor radionuclide therapy. The facility with the largest experience with ^{177}Lu is probably the Erasmus Medical Center in Rotterdam performing yearly 400 treatments with DOTATATE each comprising 200 mCi of ^{177}Lu [17]. DOTATATE is used for therapy in patients with somatostatin receptor-positive tumors, e.g. neuroendocrine tumors [18, 19, 20].

In radioimmunotherapy, ^{177}Lu is used for labeling monoclonal antibodies, most frequently bombesin analogues [21, 22, 23]. Bombesin is an analogue of the human gastrin releasing peptide (GRP) that binds to GRP receptors with high affinity and specificity. The GRP receptors are over expressed on a variety of human cancer cells including prostate, breast, lung, and pancreatic cancers [24, 25, 26].

2.2.2 Production ways

Two alternative production routes are generally applied to obtain ^{177}Lu, namely the direct route based on neutron irradiation of lutetium targets or the indirect route based on neutron irradiation of ytterbium targets followed by radiochemical separation of ^{177}Lu from ytterbium isotopes. Both routes have been under investigation

and discussion in the last years. Figure 2.2 shows the cut-out from the Chart of Nuclides showing the isotopes of ytterbium and lutetium, which are of interest. Data characterizing the activation of natural lutetium and ytterbium isotopes in a nuclear reactor and the decay of the activation products are summarized in Tab. 2.2.

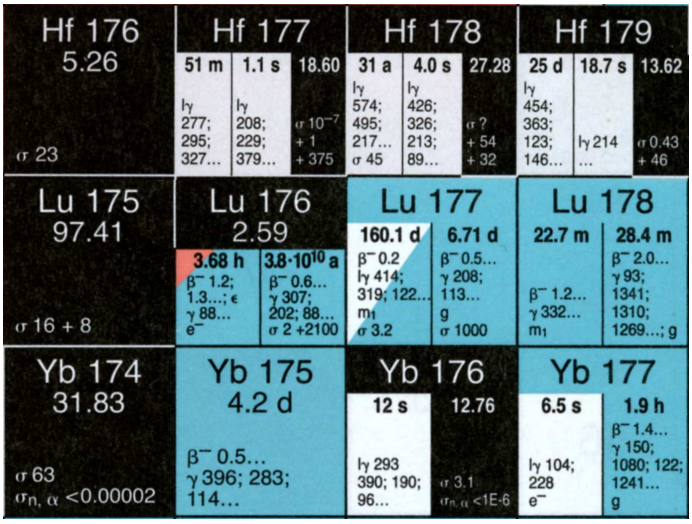

Figure 2.2: Cut-out from the Chart of Nuclides [27] showing the isotopes of ytterbium and lutetium.

Direct production route: ^{176}Lu (n,γ) ^{177}Lu

Because of the rather large cross section, ^{177}Lu can be produced directly with a relatively high specific activity by neutron capture on ^{176}Lu in nuclear reactors. Figure 2.3(a) shows the excitation function of this reaction, where a strong resonance at 0.1413 eV [28] extending to the thermal neutron region is evident. Consequently, the effective cross section of the activation reaction is even higher than the tabulated one. By irradiation of a ^{176}Lu target, a long-lived isomer is co-produced by the competing ^{176}Lu$(n,\gamma)^{177m}$Lu reaction (excitation function is given in Fig. 2.3(b)), which lowers the radionuclidic purity of ^{177}Lu preparations obtained and complicates the disposal of radioactive ^{177}Lu waste in hospitals [17]. Enriched target material is required for this production route since the natural abundance of ^{176}Lu is only 2.6%. Lutetium oxides enriched in ^{176}Lu up to approx. 60–80% are commercially available. A limitation of the direct production route is that only carrier-added ^{177}Lu preparations can be obtained because stable ^{175,176}Lu isotopes (though burned-up to

Table 2.2: Activation data of natural lutetium and ytterbium isotopes and decay data of their activation products. Data are taken from Ref. [27] for natural abundances, Ref. [28] for cross sections, Refs. [29, 30, 31, 32] for half-lives and decay modes, and Ref. [15] for γ rays and intensities

Element	Atom. mass	Abund., %	σ_0, barn	Activation product	$T_{1/2}$	Decay product(s)	Main γ rays, keV (absolute intensity, %)
Lu	175	97.41	16.7 ± 0.4	^{176m}Lu	3.664 h	^{176}Hf	88.36(8.9)
			6.6 ± 1.3	^{176}Lu	4×10^{10} y	^{176}Hf	88.34(14.5), 201.83(78.0), 306.78(93.6)
	176	2.59	317 ± 58	^{177m_1}Lu	6 min	β^-/IT=?	not known
			2.8 ± 0.7	^{177m_2}Lu	160.44 d	^{177}Hf (78.6%), ^{177}Lu (21.4%)	112.95(21.9), 128.5(15.6), 153.28(17.0), 204.11 (13.9), 208.37(57.4), 228.48(37.2), 281.79 (14.2), 327.68(18.1), 378.5(29.9), 418.54(21.3)
			2020 ± 70	^{177}Lu	6.647 d	^{177}Hf	112.95 (6.17), 136.72 (0.05), 208.37 (10.36), 249.67 (0.20), 321.32 (0.21)
Yb	168	0.13	2300 ± 170	^{169}Yb	32.026 d	^{169}Tm	63.12 (44.2), 109.78 (17.5), 177.21 (22.2), 197.96 (35.8), 307.74 (10.1)
	170	3.04	9.9 ± 1.8	^{171}Yb	stable		
	171	14.28	58.3 ± 3.8	^{172}Yb	stable		
	172	21.83	1.3 ± 0.8	^{173}Yb	stable		
	173	16.13	15.5 ± 1.5	^{174}Yb	stable		
	174	31.83	63.2 ± 1.5	^{175}Yb	4.185 d	^{175}Lu	282.52(6.1), 396.33(13.2)
	176	12.76	2.85 ± 0.05	^{177}Yb	1.911 h	^{177}Lu	150.3(20.5), 1080.5(5.9), 1241.8(3.5)

some extent) are present in the target. The maximum obtainable specific activity, that can be achieved only with high-flux reactors, is about 70% of the theoretical one.

Indirect production route: ^{176}Yb (n,γ) ^{177}Yb $\xrightarrow{\beta^-}$ ^{177}Lu

As an alternative production route, ^{177}Lu can be obtained virtually carrier-free from beta decay of ^{177}Yb produced by neutron capture on ^{176}Yb in a nuclear reactor. Figure 2.4 shows the excitation function of the ^{176}Yb$(n,\gamma)^{177}$Yb reaction. To suppress the formation of ^{169}Yb and ^{175}Yb isotopes and to increase the effectivity of the process, enriched target material is required. Ytterbium oxides enriched in ^{176}Yb up to $\approx 97\%$ are commercially available. It is in principle feasible to recycle the irradiated target because the cross section of ^{176}Yb is low and practically no target burn-up occurs, but this possibility has not been described in the literature yet. To obtain *n.c.a.* ^{177}Lu of maximum specific activity, lutetium must be separated from the ytterbium target, because ytterbium competes with lutetium in complexation during the radiopharmaceutical production. In the last years, methods for the separation of *n.c.a.* ^{177}Lu from large amounts of ytterbium have been intensively studied, resulting in the publication of several papers [34, 35, 36, 37, 38].

Practical experience with the production of ^{177}Lu

One of the first facilities where the production of ^{177}Lu was studied is the Oak Ridge National Laboratory (ORNL) in U.S.A. operating one of the world's highest flux reactor-based neutron source (the High Flux Isotope Reactor, HFIR). Both production ways were under evaluation at ORNL in 1995 [39]. Initially, lutetium or ytterbium oxide targets were irradiated for one hour in a thermal neutron flux of 2.05×10^{15} cm^{2}s^{-1} and were not processed chemically. The average ratio of experimental to theoretical yields of ^{177}Lu was found to be 1.66, when natural Lu_2O_3 or $^{176}Lu_2O_3$ of 44.2% enrichment were irradiated, and 0.79, when $^{176}Yb_2O_3$ of 96.4% enrichment were irradiated. According to calculations, the maximum yield using the direct route will be achieved after four days of irradiation at HFIR and the expected specific activity is 80 Ci/mg of ^{176}Lu (72% of the theoretical value). The fraction of ^{177m}Lu at EOB is expected to be $< 0.01\%$. The authors conclude, that if a sep-

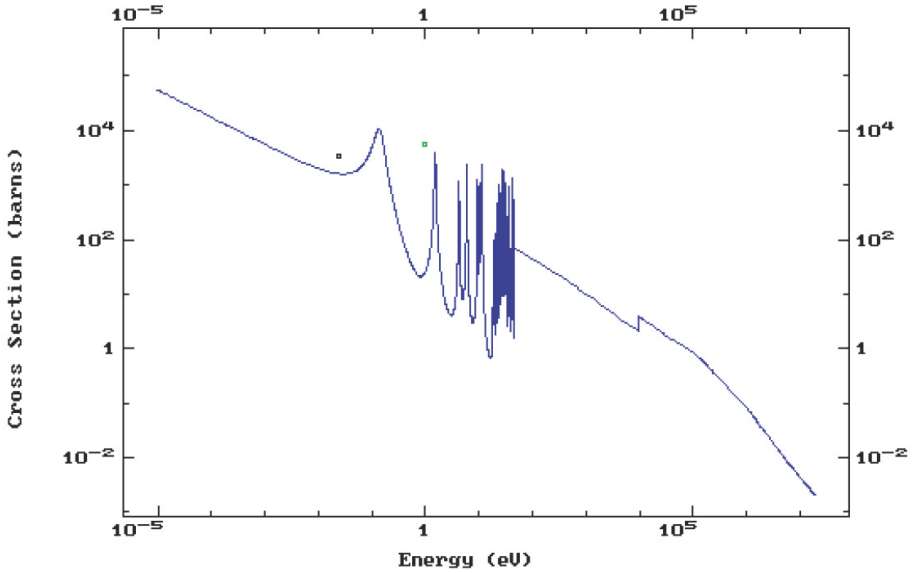

(a) ^{176}Lu (n,γ) ^{177}Lu reaction.

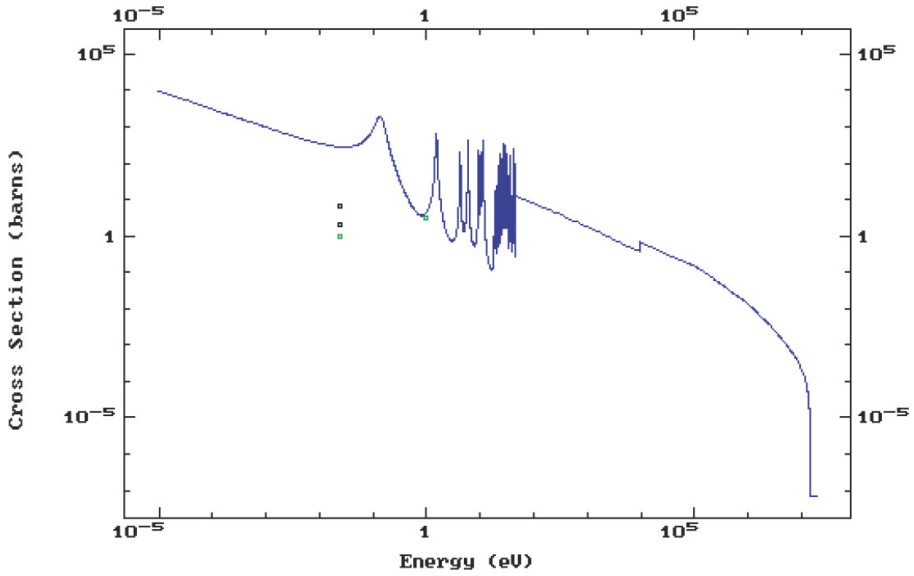

(b) ^{176}Lu (n,γ) $^{177\mathrm{m}}$Lu reaction.

Figure 2.3: Calculated excitation function of the ^{176}Lu(n,γ) reaction. Qualitatively, the character of both functions is similar, however, the formation of $^{177\mathrm{m}}$Lu is much less probable. Cross sections of both reactions exhibit a distinct resonance at $\sim$0.15 eV, extending to the thermal neutron region (energy of thermal neutrons is 0.025 eV). Because the $\sigma(E_n)$ function is not linear as $1/E_n$ in the thermal neutron region, ^{176}Lu is called a non-$1/v_n$ nuclide. The points in the graphs (at 0.025 eV and 1 eV) are experimental values. Reproduced from [33].

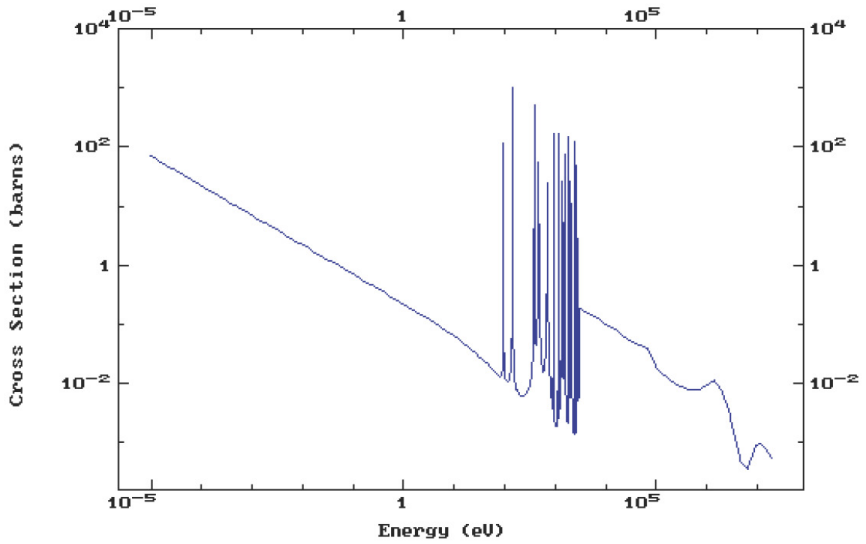

Figure 2.4: Excitation function of the ^{176}Yb (n,γ) ^{177}Yb reaction. Because the $\sigma(E_n)$ function is in the thermal neutron region linear as $1/E_n$, ^{176}Yb belongs to the $1/v_n$ nuclides. Reproduced from [33].

aration factor of ^{177}Lu from the ytterbium target of 10^6 can be achieved, then the specific activity of ^{177}Lu from both routes will be almost the same. After evaluation of the first results, specialists at ORNL focused on developing a Lu/Yb separation method based on extraction chromatography, which will be described in the next section. However, extraction chromatography was found to be not a suitable method for a Lu/Yb separation and the direct production route was evaluated as "the only practical route to provide high multi curie levels of high specific activity ^{177}Lu at ORNL" [40].

The only other facility in the world where the neutron flux is comparable with that available at HFIR ORNL is the SM reactor at Dimitrovgrad in Russia. Direct and indirect production of ^{177}Lu was studied at the State Scientific Center of Russian Federation Research Institute of Atomic Reactors (SSC RIAR), Dimitrovgrad. Both production ways were evaluated theoretically and the authors concluded that the indirect production route is the preffered one [41]. The indirect production route was studied experimentally. Targets of ^{176}Yb with 95.15% enrichment were purified from lutetium impurity before the irradiation in the SM reactor with a neutron flux of $\sim 2 \times 10^{15}$ cm^{-2}s^{-1}. Lutetium-177 was extracted from the irradiated targets by electroreduction of ytterbium on a mercury-pool cathode from lithium citrate solu-

tion. Cation exchange and extraction chromatography were used for the subsequent purification of ^{177}Lu. The radiochemical processing took about 50 hours. The reported specific activity of the product was 92.7 Ci/mg Lu (83% of the theoretical value) at EOB [41].

The production of ^{177}Lu based on the irradiation of natural and enriched lutetium and ytterbium targets was studied experimentally at the Radioisotope Centre POLATOM in Otwock-Swierk, Poland [42]. Samples consisting of lutetium or ytterbium oxides or nitrates sealed in quartz ampoules were irradiated for 5 or 10 hours in a thermal neutron flux of 2×10^{14} cm^{-2}s^{-1}. Irradiated samples were opened by cutting with diamond saw and dissolved in 1 M HNO_3. The measured yield of ^{177}Lu was found to be 14–70% higher than the theoretical one when ^{176}Lu targets of 68.9% enrichment were irradiated. In the case of the indirect production route, experimental yields were 10–25% lower than the theoretical ones when natural ytterbium was irradiated and 10–25% higher when ^{176}Yb targets of 95.2% enrichment were irradiated. The ^{177m}Lu to ^{177}Lu activity ratio was found to be 0.006% and the specific activity 15.5 Ci/mg after 9 days of irradiation [43]. It was found that the chemical purity of ^{177}Lu produced in the direct route strongly depends on the way how the irradiated quartz ampoules are opened. Opening the ampoules by cutting with a rotating diamond saw resulted in product contaminated with Ca, Cu, Fe, Mg, Pb, and Zn, so that the ^{177}Lu preparation was not acceptable for use in nuclear medicine. When the ampoule was opened by simple mechanical breaking, the chemical purity of the product was satisfactory [43]. Extraction chromatography was studied for the separation of ^{177}Lu from irradiated ytterbium targets. Satisfactory separation factors were obtained when the Yb/Lu mass ratio was < 100, but problems were encountered when scaling up to Yb/Lu mass ratios of several thousands [44].

The direct production route was evaluated in detail at the Bhabha Atomic Research Centre in Mumbai, India. In the first study [45], natural or enriched (60.6% enr.) lutetium oxides sealed in quartz ampoules were irradiated for 3–7 days at a thermal neutron flux of $\sim 3 \times 10^{13}$ cm^{-2}s^{-1}. The irradiated targets were dissolved in 1 M HCl by gentle warming. The experimental ^{177}Lu yields were found to be 40–100% higher than the calculated ones. The average content of ^{177m}Lu was found to be 0.015% at EOB. In a later study [46], $^{176}LuCl_3$ targets with 64.3% enrichment were irradiated for 7–21 days at thermal neutron fluxes of 1.4×10^{13}–1.0×10^{14} cm^{-2}s^{-1}. The experimental specific activities were found to be 2.5–2.8 times higher than ex-

pected from calculation and were up to 23 Ci/mg (21 days of irradiation at 1.0×10^{14} $cm^{-2}s^{-1}$). The ^{177m}Lu to ^{177}Lu activity ratio was 0.025% at EOB.

Relatively high specific activity ^{177}Lu is commercially available from MDS Nordion, Ottawa, Canada [47]. The specifications of the product are: specific activity $\geq$ 45 Ci/mg of lanthanides, radionuclidic purity $\geq$ 99.9%, $\leq$ 0.1% ^{175}Yb. It is produced by the indirect production route at the National Research Universal (NRU) reactor at the Chalk River Laboratories (CRL) site in Canada, where the maximal available thermal neutron flux is 3×10^{14} $cm^{-2}s^{-1}$. Which Lu/Yb separation method is used was not published.

In addition to the described reactor-based production methods, production of ^{177}Lu by deuteron induced reactions on ytterbium targets was explored at the cyclotron of the Vrije University Brussel, Belgium [48]. The following reaction is responsible for the formation of the majority of the desired nuclei: ^{176}Yb (d,p) ^{177}Yb $\xrightarrow{\beta^-}$ ^{177}Lu. Two natural ytterbium targets (12 μm thick) were irradiated with deuteron beams of 21 or 15 MeV. The authors claim that up to 30 GBq of ^{177}Lu can be produced in a 72-hour irradiation with 21 MeV deuterons (100 μA beam, 100μm thick enriched targets). However this production route seems to be not interesting because the yields are very low and Lu/Yb separation is required.

Summary

As can be seen from the presented examples, ^{177}Lu can be produced by direct and indirect production routes. The decision which production route will be employed is governed in particular by the required specific activity of the product. Further, the availability of isotopically enriched targets, the available thermal neutron flux, and the existence of an effective Lu/Yb separation method are critical. Usually, highly isotopically enriched lutetium or ytterbium targets sealed in quartz ampoules are irradiated in the form of oxides or nitrates. It has been rather the rule than the exception that the experimentally determined yields of ^{177}Lu produced in the direct route exceeded the theoretical ones by up to 180%. It is obvious that a more accurate calculation of the irradiation yield is required in order to be able to plan the production more reliably. The content of the long-lived ^{177m}Lu impurity in ^{177}Lu produced by the direct route was in general in the range of 0.01–0.025% (ratio of

^{177m}Lu and ^{177}Lu activities at EOB). This value can be reduced by applying shorter irradiation times and is independent of the target enrichment. The obtained specific activities depend strongly on the thermal neutron flux, enrichment, and production route employed. They are up to $\sim$80–90 Ci/mg in the case of ^{177}Lu produced at high-flux reactors (HFIR and SM reactor) either by the direct or the indirect route. The SSC RIAR (Russia) and CRL (Canada) are currently probably the only two facilities that routinely produce ^{177}Lu via the indirect route. Elsewhere, the direct route is employed and the specific activities are up to $\sim$15–25 Ci/mg. In general, the implementation of the indirect production route is inhibited by the unavailability of an effective separation method. The development of a suitable Lu/Yb separation process was one of the aims of the present dissertation. Methods and processes which were already studied or proposed for Lu/Yb separation are reviewed in the next section.

2.3 Separation of *n.c.a.* ^{177}Lu from an Yb target

Lutetium produced via the indirect production route has to be separated from the irradiated ytterbium target. The quality of the ^{177}Lu preparation obtained in such a process strongly depends on the employed separation method. In the ideal case, the *n.c.a.* ^{177}Lu preparation contains negligible amounts of ytterbium or stable lutetium isotopes or other radionuclidic as well as chemical impurities.

2.3.1 Requirements

Lutetium is the heaviest lanthanide and ytterbium is its lighter neighbor. In general, all lanthanides behave chemically very similar and the separation of two neighbors is a difficult task. The challenges posed by separating adjacent trivalent lanthanides have been well documented [49, 50]. Lutetium and ytterbium both exist in solution in trivalent oxidation state, however, ytterbium can be, under special conditions, reduced to the plus two state. The main reason greatly complicating the separation is, however, the presence of ytterbium in macro quantities (tens of milligram), while lutetium is found in the target only at microgram levels. Depending on the irradiation conditions and target material characteristics, the mass ratio of ytterbium to lutetium

can be in the range of several hundreds to several thousands. With regard to the intended lutetium application the requirements on the separation are quite strict:

- Reduction of the amount of ytterbium down to < 100 ng, implying decontamination factors from ytterbium higher than 10^6.
- Very high chemical (< 500 µg of metals like Ca, Cu, Zn, Al, Fe, Pb per 1 Ci of ^{177}Lu) and radionuclidic purity (< 0.1% ^{175}Yb) of the lutetium fraction.
- High recovery of lutetium (ideally > 85%).
- Lutetium should be obtained in a suitable chemical form for the labeling of radiopharmaceuticals (preferably $LuCl_3$ in 0.05 M HCl).
- It is desirable to recover and reuse the ytterbium target for the next irradiation.
- The separation process should be fast, reliable, and reproducible.
- The separation process should be adaptable to scale-up and remote handling.

2.3.2 Separation processes proposed in the literature

There are a number of separation methods described in the literature for the separation of individual lanthanides which are based mostly on ion-exchange chromatography, solvent extraction or extraction chromatography. Some works also focus on the problem of macro-micro separation of lanthanides.

Processes based on ion-exchange chromatography with α-HIB

Already fifty years ago, a separation of individual lanthanides by elution of their complexes from a cation-exchange column with α-hydroxyisobutyric acid (α-HIB, 2-hydroxy-2-methylpropanoic acid) has been described [51]. However, the separation factor α (ratio of α-HIB complex stability constants) for the Lu/Yb pair, which is the most difficult to separate among the lanthanides, is only 1.54 [52]. The advantage of the cation-exchange method is that lutetium elutes before ytterbium, which is present in much higher amounts. In the case of reversed elution order, the lutetium fraction would contain too much ytterbium because of the peak tailing. The disadvantage of

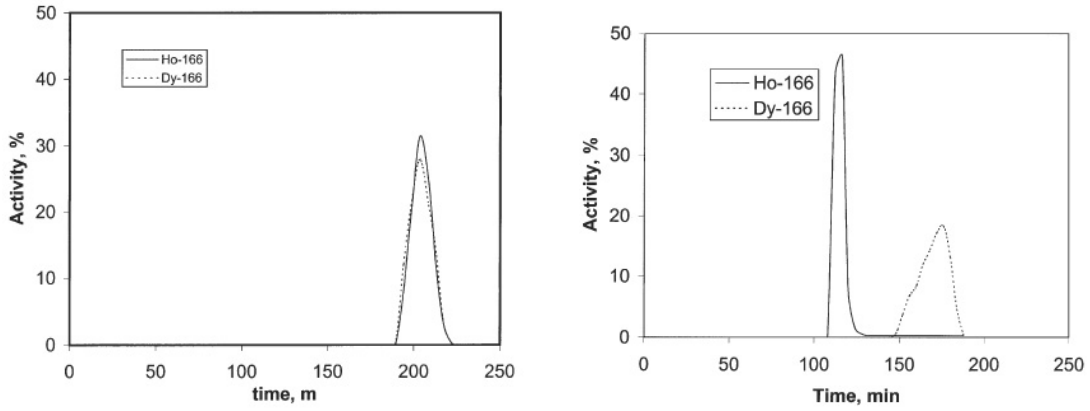

(a) Dowex 50 (b) Aminex A-7

Figure 2.5: Separation of *n.c.a.* ^{166}Ho from irradiated 1-mg Dy_2O_3 targets using (a) Dowex 50 or (b) Aminex A-7 cation-exchange resins. Reproduced from [54].

cation-exchange methods is that in general lutetium is eluted with large volumes of eluent which may increase the content of chemical impurities in the final product. Also, when α-HIB is used for elution, then as a final step, the lutetium complex with α-HIB has to be destroyed. This is accomplished by adsorption on a cation exchanger followed by elution with $\approx 9\,\mathrm{M}$ HCl [53]. Higher separation factors can be obtained using ethylenediaminetetraacetate or 1,2-diamino-cyclohexanetetraacetate (for both $\alpha = 1.7$) as eluting agents, but these systems have solubility problems and in order to recover the lanthanide from the eluate further processing is necessary [52].

Lahiri et al. studied the separation of *n.c.a.* ^{166}Ho from milligram quantities of irradiated Dy_2O_3 targets using HPLC with Dowex 50W-X8 (200–400 mesh) or Aminex A-7 (7–11 μm) cation exchangers and 0.1 M α-HIB of pH 4.2 as an eluent [54]. The therapeutic radionuclide ^{166}Ho is produced from dysprosium, the ninth lanthanide, by double neutron capture. The Ho/Dy pair represents an analogy to the Lu/Yb pair. As can be seen from Fig. 2.5, the ^{166}Ho could be quantitatively separated from the dysprosium target (1 mg) using the Aminex resin, while no separation was observed using the Dowex resin. Unfortunately, the Aminex A-7 resin is no longer commercially available. Also, a question remains about the possibility to scale-up the separation to $\sim 50\,\mathrm{mg}$ target material.

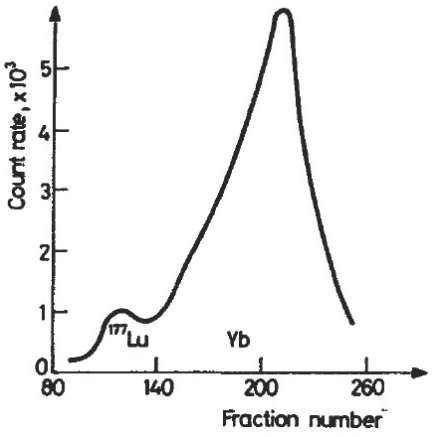

Figure 2.6: Elution profile for the Lu/Yb pair absorbed on a Dowex 50W-X8, 200-400 mesh, 33 cm × 0.7 cm cation-exchange column, using Zn^{2+} as the barrier-ion. Eluent is 0.04 M α-HIB at pH 4.6. Each fraction corresponds to 1 ml of the eluent. Reproduced from [34].

There are only few reports on the use of ion-exchange chromatography for the separation of trace amounts of lutetium from an ytterbium target. Balasubramanian describes the separation of ^{177}Lu from 10.35 mg of ytterbium using a cation exchanger Dowex 50W-X8 (200–400 mesh) in Zn^{2+} form and 0.04 M α-HIB of pH 4.6 for elution [34]. Lutetium-177 was separated with 68% yield, the purity was better than 99%, and the time required was about 4 hours. It can be seen from Fig. 2.6 that a relatively pure lutetium fraction could be obtained only if more than 30% of lutetium, which was contaminated with ytterbium, was sacrificed. This method has even more drawbacks: the separated lutetium is highly diluted in large volumes of eluent and it is contaminated with the barrier-ion Zn^{2+}.

Hashimoto et al. optimized the reversed-phase ion-pair chromatography for the separation of *n.c.a.* ^{177}Lu from irradiated Yb_2O_3 targets [36]. The activity was loaded on a Resolve C18 column and then eluted with a mixture of 0.25 M α-HIB as complexing agent and 0.1 M 1-octanesulfonate as ion-pairing agent. It is obvious from Fig. 2.7 that complete separation was achieved only when the ytterbium amount was less than 1 mg. As the amount of Yb_2O_3 was increased from 0.01 to 5 mg, the ytterbium peak leaned toward the lutetium peak and the separation efficiency got worse. It follows that this method is unsuitable for the production of ^{177}Lu for medical applications.

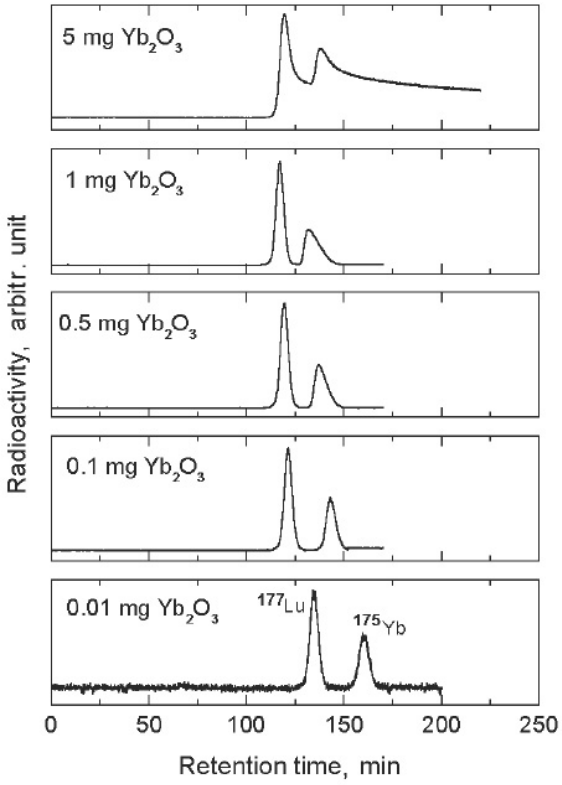

Figure 2.7: Effect of the amount of Yb_2O_3 on the separation efficiency of the Lu/Yb pair. Column: 0.8 cm $\times$ 30 cm Resolve C18 Radial-Pak; eluent: 0.25 M α-HIB/0.1 M 1-octanesulfonate; flow rate: 2 ml/min. Reproduced from [36].

Processes based on extraction chromatography

The second group of methods employs solvent extraction or extraction chromatography based on the different extractability of lanthanides with acidic organophosphorus extractants. The separation of individual lanthanides by means of extraction chromatography was intensively studied by E. P. Horwitz [55, 56], eventually producing the LN Resin, which is available from Eichrom Technologies, Inc. [57]. The extractant used in LN Resin is di(2-ethylhexyl) orthophosphoric acid (HDEHP).

Mirzadeh and Knapp made use of the commercially available LN Resin in a patented "method for preparing high specific activity ^{177}Lu" [37, 58]. In a one-step chromatography process, the *n.c.a.* ^{177}Lu was quantitatively separated from 10 mg of ytterbium by elution with increasing concentrations of HCl (Fig. 2.8). The authors

claim that the specific activity of thereby obtained ^{177}Lu will be at least 100 Ci/mg Lu (i.e. 91% of the theoretical one). Unfortunately, the separation yield and purity were not published. Knapp et al. also observed that Lu/Yb could not be eluted from LN Resin using HNO_3 with concentrations up to 2 M [58], as recommended by the manufacturer (consult [57]).

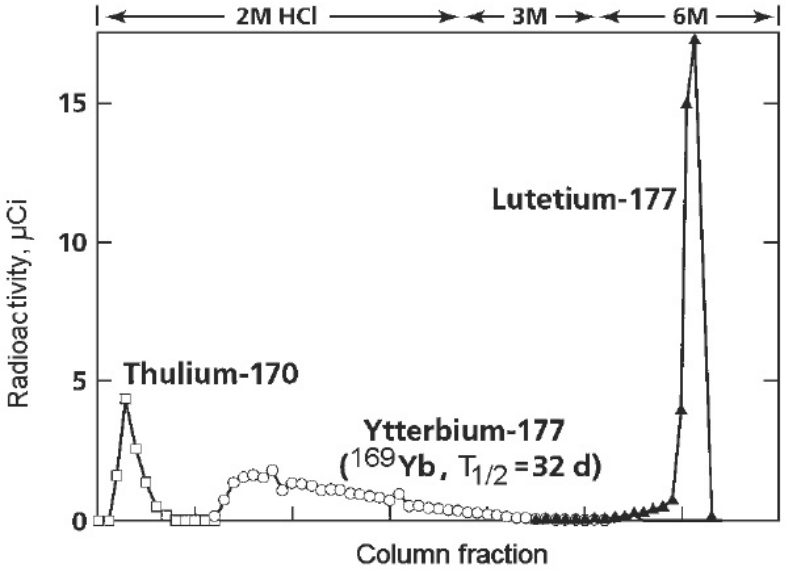

Figure 2.8: Separation of ^{177}Lu from ytterbium using the Eichrom LN Resin eluted with increasing concentrations of HCl. Reproduced from [58].

Eichrom process The inventor of the LN Resin, E. P. Horwitz, reacted promptly upon Mirzadeh's patent publication [37] and developed a conceptual flowsheet for the separation of *n.c.a.* ^{177}Lu from a 300 mg irradiated ytterbium target [38]. Even though, several different extraction-chromatographic resins are employed in a multi-step process (see Fig. 2.9), the flowsheet has some very interesting features and seems to be effective even for bulkier ytterbium targets. The separation takes place on the LN2 Resins, while the DGA Resins serve for the reduction of sample volume, acidity adjustment and purification from chemical impurities. The LN2 Resin is an improved LN Resin containing (2-ethyl-1-hexyl)phosphonic acid mono (2-ethyl-1-hexyl) ester as extractant and the polymeric support is of 25–53 μm particle size range. The task of the UTEVA resin is to bond traces of the extractant leaching off of the LN2 Resins and causing problems when stripping the DGA Resin. The

anion-exchange resin employed as the final step in the separation scheme eliminates all traces of nitrate ions in the eluate so that the lutetium is obtained in 0.05 M HCl.

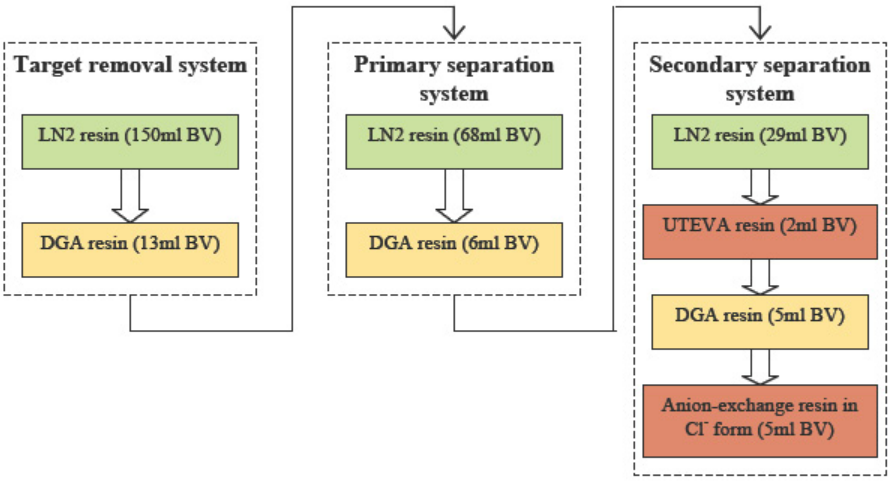

Figure 2.9: The separation scheme proposed by Horwitz [38] for the separation of *n.c.a.* ^{177}Lu from irradiated ytterbium target. BV is bed volume.

The advantage of the proposed separation process is the possibility to run the columns in tandem without any evaporation steps or acidity adjustments in between. The process is characterized by a separation yield of 73% ^{177}Lu and a decontamination factor from ytterbium of 10^6. A typical elution profile from the LN2 Resin is shown in Fig. 2.10 from where it is obvious that some method of on-line detection is necessary to accurately determine the cuts for the Yb- and Lu-rich fraction. Probably the most serious shortcoming of the outlined process is its price because due to leaching of the extractant and radiolytic degradation, the LN2 Resin can be used only once and the DGA Resin only three times. It follows that each separation (with $\sim$300 mg target) requires on average 250 ml of fresh LN2 Resin and 7 ml of fresh DGA Resin (the prices are: 365 Euro for 10 g of LN Resin, 175 Euro for 10 g of DGA Resin [57]).

Redox processes

The last group of separation methods suitable for the separation of individual lanthanides comprises processes which exploit the ability of some lanthanides to exist

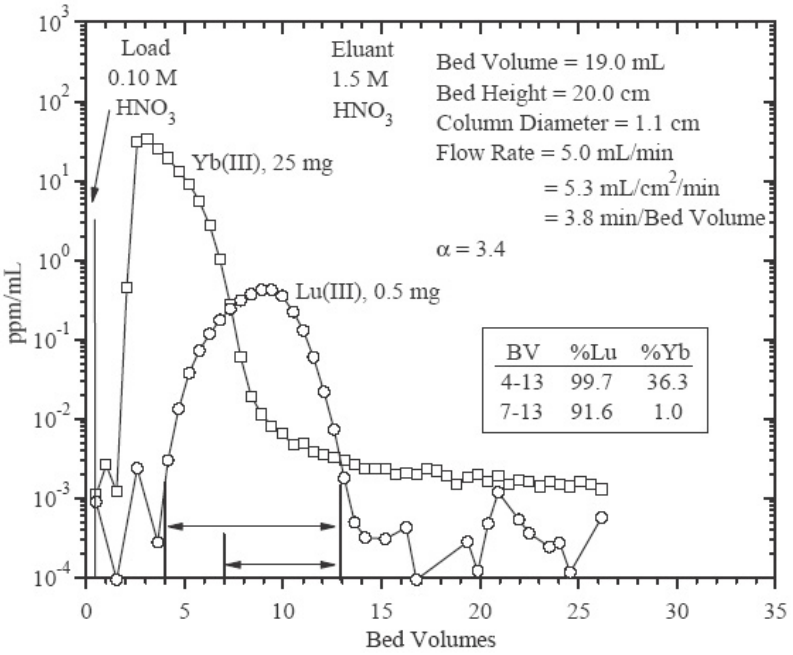

Figure 2.10: Separation of *n.c.a.* ^{177}Lu from 25 mg ytterbium target on LN2 Resin (19 mL BV) using 1.5 M HNO_3, 4.8% of the total column capacity is used. Reproduced from [38].

in other oxidation states than (III). For example, cerium can be tetravalent under certain conditions, while europium, ytterbium, and samarium exist in the bivalent state.

Cementation process The separation of different lanthanides with sodium amalgam was first described by Marsh [59, 60, 61, 62] and further experiments were done later by Barrett et al. [63], Lawless et al. [64], Novgorodov et al. [65], and Denzler et al. [53]. The so called cementation process was optimised for the separation of *n.c.a.* ^{177}Lu from 200 mg ytterbium target by Lebedev et al. [35]. It is based on the selective reductive separation of ytterbium with sodium amalgam followed by cation-exchange purification. The reduction is described by the following reaction:

$$Yb^{3+} + Na \rightleftharpoons Yb^{2+} + Na^{+}$$

During the cementation process, the irradiated Yb_2O_3 is dissolved in hydrochloric acid, sodium acetate is added and the solution is stirred with sodium amalgam for

90 s. After that, amalgam containing the separated ytterbium is removed from the system. The cementation step has to be repeated four times in order to separate 99% of ytterbium. Lutetium and remaining ytterbium are then coprecipitated with lanthanum as hydroxides, redissolved and separated using a cation-exchange column and α-HIB as eluent. In the last step, the lutetium complex is destroyed by absorption on a cation-exchange column and elution of lutetium with 9 M HCl. In this process, lutetium can be obtained with a separation yield of 75% and decontamination factor from ytterbium of $> 10^6$. However, special attention has to be paid to the removal of mercury compounds which are introduced into the lutetium fraction during the mixing with amalgam.

2.3.3 Summary

The employment of ion-exchange chromatography, extraction chromatography, and redox processes has been considered for the recovery of micro amounts of ^{177}Lu from neutron-irradiated ytterbium targets.

Ion-exchange chromatography has an advantage over extraction chromatography in that lutetium elutes before ytterbium, which is present in much higher amounts. Unfortunately, the separation factors are very low and only resins fulfilling certain requirements result in satisfactory separations. Cation-exchange chromatography with the complexing eluent α-HIB was found to be most efficient when strong cation-exchange resins like Aminex from Bio-Rad laboratories, U.S.A. were employed [54, 66]. The Aminex resins excel in small spherical beads with very narrow particle size distribution (e.g. Aminex A-5: $13 \pm 2\,\mu$m, Aminex A-7: 7–11 μm, Aminex A-9: $11.5 \pm 0.5\,\mu$m) and the ability to withstand high pressures up to 1500 psi ($\approx$ 100 bar) [67]. This makes them predestined for such demanding tasks such as the separation of individual lanthanides with the application of HPLC. Unfortunately, the Aminex resins are no longer produced and no other resin of similar qualities is commercially available, at present. It follows that ion-exchange chromatography is currently not used for the primary separation of ^{177}Lu from the target. Instead, it is often employed for the final purification of a pre-separated ^{177}Lu fraction (e.g. in the cementation process).

It has been shown that extraction chromatography can be successfully applied

for the separation of ^{177}Lu from the ytterbium target. Processes based on extraction chromatography were employed at the University of Missouri Research Reactor Center (MURR), at HFIR ORNL, and at the Radioisotope Centre POLATOM. Unfortunately, it was recognized that these processes are very time consuming, expensive, and generating large volumes of radioactive waste. Problems to meet the chemical purity requirements were also reported [44]. Other separation methods are investigated at MURR. Currently, the extraction of lanthanide-polyoxometalate complexes from aqueous solution into chloroform containing amines is studied [68]. Specialists at ORNL came to the conclusion that the extraction chromatography is not suitable for a Lu/Yb separation [40]. At POLATOM, insufficient separation factors were obtained when scaling up the separation to Yb/Lu mass ratios to be expected in irradiated targets [44]. Thus, extraction chromatography can be used (at higher costs and work demand) at high flux reactors where the Yb/Lu mass ratio in the target is lower, but is not suitable for low and moderate flux reactors.

The most efficient separation method available at present is probably the cementation process exploiting the ability of ytterbium to be reduced to the divalent state. The cementation process is employed for the recovery of ^{177}Lu from ytterbium targets irradiated at the high-flux SM reactor at SSC RIAR. However, only little information describing the practical experience with this process has been published. Unfortunately, the cementation process is not easily accepted by physicians, because there exists a danger of mercury compounds being present in the final ^{177}Lu preparation, which could have fatal consequences.

Chapter 3

Experimental

This chapter describes in detail the experimental techniques and procedures employed throughout this work, as well as chemicals and instruments used. Theoretical concepts and relations necessary for understanding the calculations carried out in Chapter 4 are introduced here.

3.1 Experimental methods and techniques

3.1.1 Research reactors as a tool for radionuclide production

In nuclear reactors, radioisotopes are produced mostly by (n, γ) reactions, so they are neutron rich and decay by emission of β^- particles. Not every nuclear reactor is, however, suitable for the production of radionuclides. Nuclear reactors may be divided into two basic groups: power reactors, whose primary function is to produce heat to generate electricity, and research reactors, which provide neutrons for research and other purposes. One of the biggest advantage of research reactors is their clean thermal neutron spectrum with only a small fraction of fast neutrons, which could induce $(n, 2n)$, (n, p), or (n, α) reactions and thus contaminate the product.

Neutron spectrum Neutrons formed in the reactor have a continuous energy spectrum extending approx. from 0.01 to 20 MeV. Reactor neutrons are classified accord-

ing to their energy into three groups [69]:

(a) Thermal neutrons are those which are in thermal equilibrium with molecules of the surrounding medium. They have an energy of 0.0253 eV at a temperature of 20°C. The energy distribution of this group of neutrons can be represented by a Maxwellian distribution.

(b) Epithermal neutrons are those that have been moderated to a lesser or greater extent, but have not reached thermal equilibrium. They have energies in the range of ≈ 1 eV to ~ 100 keV. The dividing line between thermal and epithermal neutrons is commonly taken as 0.55 eV (the cadmium cut-off energy). The $1/E_n$ (where E_n is the energy of neutrons) law can approximately represent the distribution of epithermal neutrons.

(c) Fast neutrons are neutrons with high energy (above 0.1 MeV). They have small significance in thermal reactors and for radioisotope production.

A typical neutron spectrum in a well-moderated reactor (such as FRM-II) is shown in Fig. 3.1.

Cross section The probability of the reaction of neutrons with nuclei is given in terms of the neutron capture cross section and is measured in units of area, given in barns ($1\,\mathrm{b} = 10^{-28}$ m^2). The (n, γ) reaction is one of the most important reactions for radionuclide production in reactors. The value of the neutron capture cross section, σ, depends on the energy of the neutrons and varies from nucleus to nucleus. In general, the slower the neutrons are, the greater is the probability for an (n, γ) reaction. In the thermal neutron region, the cross section varies as $1/v_n$, where v_n is velocity of neutrons (so called $1/v_n$ law). As the energy of neutrons increases to the epithermal region, the cross section shows a sharp variation with energy, with discrete sharp peaks called resonances. The dependence of the reaction cross section on the neutron energy is called excitation function. An example of such excitation functions are given in Figs. 2.3 and 2.4.

Choice of target material With respect to the conditions during irradiation and to further processing, the following requirements are imposed on the target material [1, 69]:

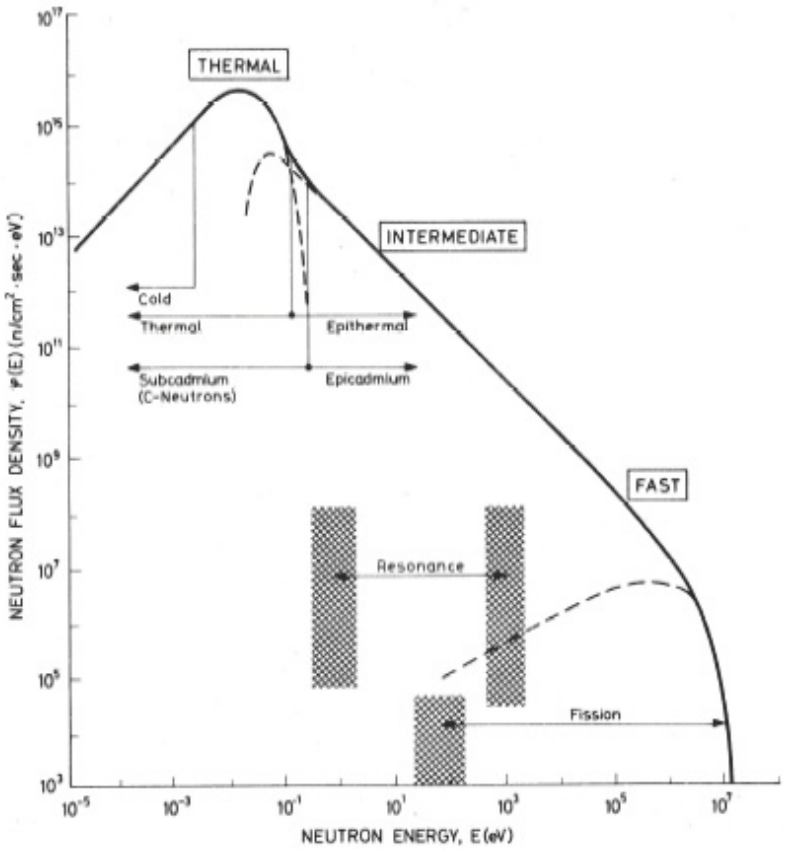

Figure 3.1: Typical neutron spectrum (neutron flux vs. neutron energy E_n) in a well-moderated reactor with different neutron energy regions - thermal, epithermal (intermediate), and fast. The area where resonances in the neutron capture cross section occur is also shown. Reproduced from [70].

- Stability under irradiation conditions.

- Good thermal conductivity and high melting point.

- Suitable chemical form to enable easy post-irradiation processing.

- High chemical purity in order to avoid production of radiocontaminants.

- Isotopically enriched target materials, if the production of radioisotopes with higher specific activity is required.

- Such a physical form of the target and target geometry that self absorption is minimal.

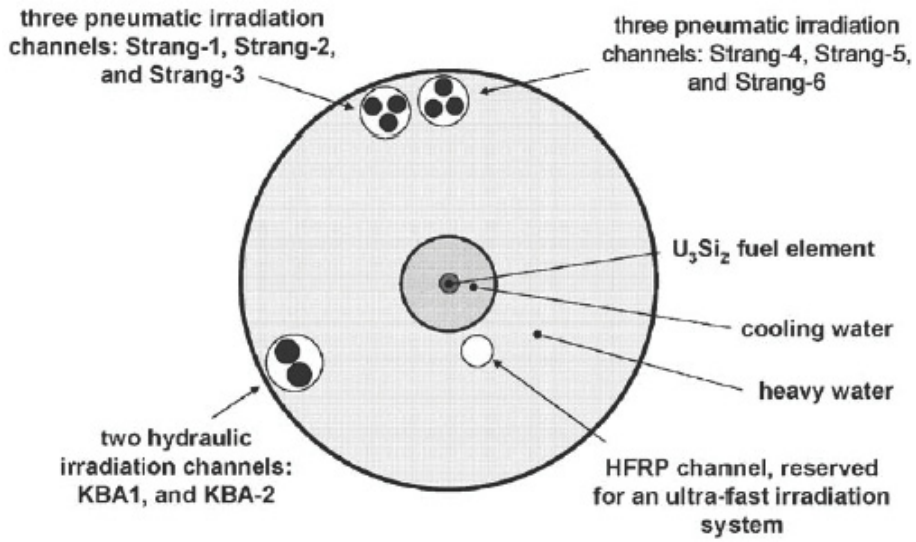

Figure 3.2: Schematic diagram of the irradiation devices in the reactor FRM-II. The irradiation channel KBA 1 was used in this work. It has the highest neutron flux after the HFRP channel. Reproduced from [71].

Research reactor FRM-II

The irradiations carried out in the framework of this dissertation were performed at the research reactor FRM-II in Garching, Germany, which was taken in operation in 2004. This reactor with 20 MW thermal power is based on a single 8-kg U_3Si_2-Al fuel element with a ^{235}U enrichment of 93%. The fuel element is cooled with light water and surrounded by heavy water (moderator and reflector) in a large moderator tank, where a high flux of thermal neutrons builds up. One reactor cycle takes $\sim$52 days, five cycles take place per year. For sample irradiation, six independent pneumatic rabbit devices and two hydraulic devices (capsule irradiation facility) are available (see Fig. 3.2). The pneumatic rabbit devices permit irradiations lasting up to a few hours with neutron fluxes varying in the range of 4.8×10^{12}–7.3×10^{13} cm^{-2}s^{-1}. Long time irradiations (up to 52 days) of larger samples (up to 30 cm^3) can be performed in the two hydraulic devices. In each hydraulic device, a maximum of 5 aluminum capsules in a stack can be irradiated simultaneously. Due to different positions relative to the reactor core, the capsules in one channel receive different neutron fluxes in the range of 7.7×10^{13}–1.3×10^{14} cm^{-2}s^{-1}.

Irradiation yield of the (n, γ) reaction

When a target isotope ${}^{A}_{Z}\mathrm{X}$ is under irradiation in a reactor, two processes occur - the radionuclide ${}^{A+1}_{Z}\mathrm{Y}$ is formed (${}^{A}_{Z}X(n,\gamma){}^{A+1}_{Z}Y$) and as soon as it is formed, it starts radioactive decay (${}^{A+1}_{Z}Y \overset{\beta^-}{\rightarrow} {}^{A+1}_{Z+1}S$). The net rate of production of a radionuclide is given by the difference of its growth and decay as expressed by the following equation:

$$\frac{\mathrm{d}N_Y}{\mathrm{d}t} = \left(\frac{\mathrm{d}N_Y}{\mathrm{d}t}\right)_{\text{growth}} + \quad \left(\frac{\mathrm{d}N_Y}{\mathrm{d}t}\right)_{\text{decay}} \tag{3.1}$$

or

$$\frac{\mathrm{d}N_Y}{\mathrm{d}t} = N_X\phi\sigma_X - N_Y\lambda_Y \tag{3.2}$$

where

N_Y	is the number of radioactive atoms Y formed,
N_X	is the number of target atoms X,
ϕ	is the neutron flux ($\mathrm{cm^{-2}s^{-1}}$),
σ_X	is the neutron capture cross section of X ($\mathrm{cm^2}$),
λ_Y	is the decay constant of Y ($\mathrm{s^{-1}}$),
t	is irradiation time (s).

Integrating equation (3.2) yields

$$N_Y = \frac{N_X\phi\sigma_X}{\lambda_Y}(1 - e^{-\lambda_Y t}). \tag{3.3}$$

The activity, A_Y (Bq), of radionuclide Y at time t is given by:

$$A_Y = N_Y\lambda_Y = N_X\phi\sigma_X(1 - e^{-\lambda_Y t}) \tag{3.4}$$

If irradiation time is much longer than the half-life of Y, $t \gg T_{1/2}$, then 3.4 gives the saturation activity:

$$A_{Y,sat} = N_X\phi\sigma_X \tag{3.5}$$

It is obvious from Eq. 3.5 that the saturation activity is limited by the neutron flux in the reactor. Equation 3.4 is the basic equation used for the calculation of the activation yield. In practice, the activity induced in the target under irradiation will be less than the activity calculated using 3.4, due to several factors, such as:

- self shielding effect in the target
- power variation in the reactor
- flux depression due to adjacent samples in the reactor especially when such samples are high neutron absorbers
- burn-up of the target material with time
- consumption of the product nucleus due to subsequent neutron capture (product burn-up).

Self-shielding effect This effect becomes predominant in case of bulkier targets with high neutron capture cross sections where the neutron flux in the volume of the target gets reduced, thereby decreasing the activity built up. In such cases, a correction factor is introduced which depends upon the geometry of the target and can be evaluated theoretically. However, it is rather difficult to arrive at a suitable correction factor for odd geometries. It is preferable to establish such factors by actual trial irradiations in the reactor.

Target burn-up and consumption of product atoms These effects become predominant in long term irradiations of targets with high neutron capture cross sections. In such cases the net rate of growth of the product nucleus Y can be written as:

$$\frac{\mathrm{d}N_Y}{\mathrm{d}t} = \left(\frac{\mathrm{d}N_Y}{\mathrm{d}t}\right)_{\text{growth}} + \left(\frac{\mathrm{d}N_Y}{\mathrm{d}t}\right)_{\text{decay}} + \left(\frac{\mathrm{d}N_Y}{\mathrm{d}t}\right)_{\text{product burn-up}} \tag{3.6}$$

or

$$\frac{\mathrm{d}N_Y}{\mathrm{d}t} = N_X\phi\sigma_X - N_Y\lambda_Y - N_Y\phi\sigma_Y \tag{3.7}$$

where

N_X is equal to $N_{X,0}e^{-\phi\sigma_X t}$, $N_{X,0}$ is the initial number of target atoms X

σ_Y is the absorption cross section of the product nucleus

If σ_Y is low, then product burn-up can be neglected and integration of 3.7 gives:

$$N_Y = \frac{N_{X,0}\phi\sigma_X}{\lambda_Y - \phi\sigma_X} \quad (e^{-\phi\sigma_X t} - e^{-\lambda_Y t}) \tag{3.8}$$

Høgdahl and Westcott conventions Until now, the reaction rate was calculated as $R = \phi\sigma$, the product of the monoenergetic neutron flux and the tabulated cross section (given for neutrons of $E_n = 0.253$ eV and $v_n = 2200$ m/s). In a reactor, both neutron flux and cross section are functions of neutron energy. The general equation describing the reaction rate is [1]:

$$R = \int \frac{\mathrm{d}(\phi\sigma)}{\mathrm{d}E}\mathrm{d}E \tag{3.9}$$

It is customary to divide Eq. 3.9 into two parts representing the contribution from thermal and epithermal neutrons:

$$R = \int_0^{5kT} \frac{\mathrm{d}(\phi\sigma)}{\mathrm{d}E}\mathrm{d}E + \int_{5kT}^{\infty} \frac{\mathrm{d}(\phi\sigma)}{\mathrm{d}E}\mathrm{d}E. \tag{3.10}$$

In neutron activation analysis, the reaction rate is calculated using the Høgdahl convention [72, 73] as:

$$R = \phi_{th}\sigma_0 + \phi_{ep}I_0(\alpha) = \phi_{th}\left(\sigma_0 + \frac{1}{f}I_0(\alpha)\right) = \phi_{th}\sigma_{eff} \tag{3.11}$$

where

ϕ_{th}	is the thermal neutron flux ($cm^{-2}s^{-1}$),
ϕ_{ep}	is the epithermal neutron flux ($cm^{-2}s^{-1}$),
σ_0	is the neutron capture cross section at $E_n = 0.253$ eV, $v_n = 2200$ m/s (cm^2),
σ_{eff}	is the effective neutron capture cross section (cm^2),
f	$= \phi_{th}/\phi_{ep}$, is the thermal to epithermal flux ratio,
$I_0(\alpha)$	is the resonance integral for $1/E_n^{1+\alpha}$ epithermal spectrum (cm^2),
α	is the shape factor of the epithermal flux (for explanation see Fig. 3.3).

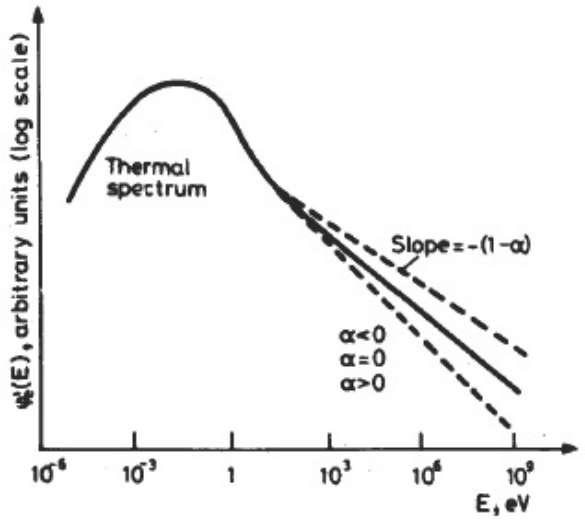

Figure 3.3: Thermal and epithermal neutron spectrum in a reactor (neutron flux vs. neutron energy E_n). Epithermal neutron flux ϕ_{ep} varies approximately as $1/E_n$ (full line in the picture). More accurately ϕ_{ep} varies as $1/E_n^{1+\alpha}$ (dashed lines), where α is the shape factor of the epithermal flux and is close to zero (it is ~ 0.06 for FRM-II). Reproduced from [74].

The Høgdahl convention requires that the neutron capture cross section varies to a good approximation as $1/v_n$ up to ≈ 1.5 eV. This requirement is met by the majority of nuclides. However, some nuclides deviate to a lesser or greater extent (e.g. ^{151}Eu and ^{176}Lu, see Fig. 3.4) [75]. For these nuclides, the modified Westcott convention, taking into account also a non-ideal epithermal flux distribution and neutron self-

shielding, has to be applied for the calculation of the reaction rate [76, 77]:

$$R = \phi_{th}\sigma_0\Big[G_{th}\cdot\, g(T_n) + G_r\,\cdot\, r(\alpha)\sqrt{\frac{T_n}{T_0}}\cdot\, s_0(\alpha)\Big] \tag{3.12}$$

where

G_{th}	is the thermal neutron self-shielding factor,
G_r	is the epithermal neutron self-shielding factor,
$g(T_n)$	is the Westcott factor with thermal neutron temperature T_n,
$r(\alpha)\sqrt{\frac{T_n}{T_0}}$	is the Westcott spectral index,
$s_0(\alpha)$	$= s_0 \cdot (\bar{E}_r)^{-\alpha}$, where s_0 and $\bar{E}_r$ are constants [78].

Irradiation yield of the (n,γ) reaction followed by β^- decay

Some radionuclides are produced by the (n,γ) reaction followed by β^- decay, which can be described by $X(n,\gamma)Y \overset{\beta^-}{\rightarrow} Z \overset{\beta^-}{\rightarrow} S$. In this case, the net production rate of nuclide Z is given by [79]:

$$\frac{\mathrm{d}N_Z}{\mathrm{d}t} = N_X(1-e^{-\lambda_Y t})\phi\sigma_X - N_Z\lambda_Z \tag{3.13}$$

If the number of target atoms, N_X, can be assumed to remain constant (no considerable target burn-up) and $N_Y = N_Z = 0$ at $t = 0$ (start of irradiation), the following equation is obtained by integration of 3.13:

$$N_Z = N_X\phi\sigma_X\left[\left(\frac{1-e^{-\lambda_Z t}}{\lambda_Z} + \frac{e^{-\lambda_Y t}-e^{-\lambda_Z t}}{\lambda_Y-\lambda_Z}\right)e^{-\lambda_Z t_d} + \frac{(1-e^{-\lambda_Y t})(e^{-\lambda_Y t_d}-e^{-\lambda_Z t_d})}{\lambda_Z-\lambda_Y}\right] \tag{3.14}$$

where t is the time of irradiation and t_d is the decay time after the end of irradiation. Other quantities have the same meaning as in the previous section. Equation 3.14 is the basic equation used for the calculation of yield of the (n,γ) reaction followed by β^- decay. It is obvious that this equation should be modified accordingly in order to account for various effects like e.g. target burn-up, self-shielding, or non-$1/v_n$ behavior, in a similar manner as was shown in the previous section.

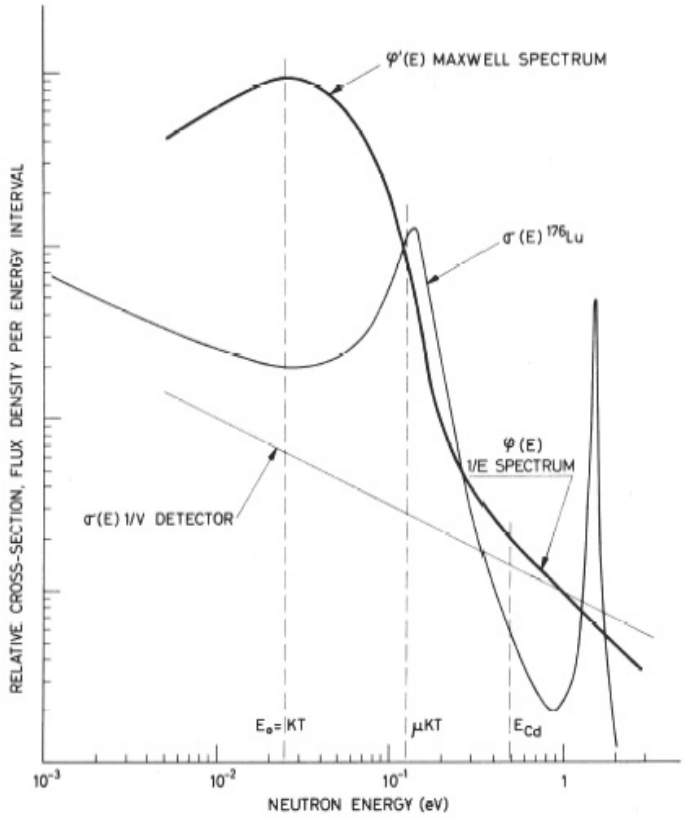

Figure 3.4: Thermal (Maxwellian) and epithermal ($1/E_n$) neutron spectrum shown by a thick line (neutron flux vs. neutron energy E_n). Furthermore, excitation functions for typical $1/v_n$ (straight line) and non-$1/v_n$ nuclides are shown (cross section vs. neutron energy). Lutetium-176 serves as an example of a typical non-$1/v_n$ nuclide. Reproduced from [70].

3.2 Experimental procedures

3.2.1 Chemicals and instruments

All reagents were used as received from commercial sources, unless noted otherwise. In all experiments and for all preparations deionized water from a Milli-Q Plus water purification system (Millipore, U.S.A.) was used. The required acid solutions were prepared by dilution of commercial concentrated HCl and HNO_3 acids. All experiments were performed at temperatures of 20 ± 2°C. Pipetting was performed with Eppendorf Research Series 2100 pipettes (Eppendorf, Germany).

The determination of the concentration of ions in sample solutions was performed with a Varian Vista-PRO CCD simultaneous inductively coupled plasma - optical emission spectroscopy instrument (ICP-OES). For the determination of isotopic compositions, a Thermo-Finnigan Element 2 high resolution inductively coupled plasma - mass spectroscopy instrument (ICP-MS) was used. The ICP-OES and ICP-MS measurements were done on request by the analytical group at our institute.

The determination of the radioactivity of the irradiated Lu/Yb targets was carried out by gammaspectrometry. Gamma-spectra were acquired using a high purity germanium detector coupled to a multichannel analyser (Canberra, Germany). The energy calibration of the detector was performed regularly by a γ-ray standard covering the energy range from 59.5 keV (^{241}Am) to 1332.5 keV (^{60}Co). Samples were measured at a distance of 15 cm from the detector. The obtained γ spectra were analysed with the help of the program MULTINAA [80] on a VAX computer.

3.2.2 Determination of neutron flux parameters

The hydraulic device receiving the highest neutron flux at FRM-II, irradiation position KBA 1-1, was used throughout this work and the neutron flux parameters at this position were determined. To accomplish this, six flux monitors (Al-Au, Al-Co, Al-Lu, Al-U, Zr, and Ni) were fixed and sealed in one quartz ampoule and irradiated in KBA 1-1 for one hour. Further, in order to monitor the eventual change of the thermal neutron flux and thermal neutron flux temperature during the reactor operation cycle, Al-Au and Al-Lu were irradiated together in KBA 1-1 for one hour several times during the cycle.

The employed flux monitors were as follows: Al-Au wire IRMM-530R with (0.1003 $\pm$ 0.0012)% Au; Al-Co wire with (0.10437 $\pm$ 0.0014)% Co or (1.0037 $\pm$ 0.012)% Co; Al-Lu wire IRMM-sp96091 with 0.1% Lu; Al-U foil IRMM-NS00017 with 0.2% U (99.9520 at.% ^{238}U); Zr-foil GoodFellow with 99.8+% Zr; and Ni-foil GoodFellow with 99.999% Ni. After the irradiation, the ampoules were opened and the activity of each monitor was measured individually at a distance of 15 cm with calibrated germanium detectors coupled to multichannel analyzers. Based on the γ-ray spectra of the activated flux monitors, the neutron flux parameters were calculated using the program MULTIFLUX [80]. Nuclear data used in the calculations are given in [71].

3.2.3 Production of ^{177}Lu

Lutetium-177 was produced by irradiation of two different target materials (^{176}Lu or ^{176}Yb) but the procedures employed for the target preparation and processing were essecially identical. The first irradiations were done with targets prepared from $^{176}Lu_2O_3$ with 64.3% of ^{176}Lu (IsoTrade, Germany). Later, $^{176}Lu_2O_3$ with 82.2% of ^{176}Lu and $^{176}Yb_2O_3$ with 97.1% of ^{176}Yb were obtained from Trace Sciences International, Canada. Characteristics of these oxides are summarized in Tab. 3.1.

Target preparation

Stock solutions of the respective isotopes were prepared by dissolution of the purchased oxides in nitric acid. This was achieved by adding small amounts of $\sim 3.5\,\mathrm{M}$ HNO_3 to the weighed oxides, warming up to $\sim 80°\mathrm{C}$ in a water bath for about 30 minutes and adjusting the acid concentration to $0.5\,\mathrm{M}$ HNO_3 by adding pure water (puriss p.a., ACS, for inorganic trace analysis; Fluka, Germany). Targets for irradiation were prepared by pipetting the stock solution (20–100 μL) into quartz ampoules, evaporating to dryness in an oven and sealing the ampoules with a flame. The 6-cm-long ampoules were prepared by the glass-blower at our institute from 1-m quartz glass tubes (Heraeus Quarzglas, HSQ 300) of 6 mm outer and 5 mm inner diameter (Vogelsberger Quarzglastechnik, Germany). They were washed by boiling in 50% HCl and washing with water before use.

Irradiation

For irradiation, three identical ampoules containing the target were wrapped in common household aluminum foil and passed to the reactor service staff who sealed the samples in a water-tight aluminum container, which was then placed in the aluminum irradiation capsule (rabbit). All discussed irradiations were performed at the Munich reactor FRM-II in the capsule irradiation facility KBA 1-1, where the thermal neutron flux is approximately $1.33 \times 10^{14}\,\mathrm{cm^{-2}\,s^{-1}}$. The irradiation times and subsequent decay times varied from several hours up to several days. The irradiated samples were collected at the reactor after certain decay times and transported to RCM in a small lead-shielded cart.

Table 3.1: Isotopic and chemical composition of purchased enriched lutetium and ytterbium oxides, according to the enclosed certificates of analysis. If "–" is given, then the data were not available or are not of relevance.

Isotope /	Isotopic distribution (%) / Concentration (ppm)		
Element	$^{176}Lu_2O_3$	$^{176}Lu_2O_3$	$^{176}Yb_2O_3$
^{176}Lu	64.3	82.2 ± 0.4	–
^{176}Yb	–	–	97.1 ± 0.1
Na	10	–	20
K	10	<50	<30
Ca	200	<50	40
Mg	30	4	–
Fe	40	<50	<20
Al	40	4	40
Zn	–	27	–
Si	40	<50	20
Cr	10	<5	–
Ni	10	–	<10
Cu	10	16	<10
Pb	10	33	30
Mn	10	14	–
Sn	10	–	<20
La	–	71	–
Ce	–	66	–
Pr	–	1	–
Nd	600	2	–
Sm	200	3	–
Eu	100	7	–
Gd	100	3	–
Dy	–	2	–
Er	–	15	80
Tm	–	<1	90
Yb	5000	5	–
Lu	–	–	90

Target processing

The activity of the irradiated samples was measured either directly in the quartz ampoules or an aliquot obtained by breaking the ampoule and dissolving its content in 0.01 M HCl was measured. Ampoules were broken in a system shown in Fig. 3.5. The heart of the system was a 6 cm long Teflon tube, called center tube hereafter (7 mm inner and 8.5 mm outer diameter), connected at both ends to Teflon tubing via tailored Teflon 1/8"-to-8mm connectors (Bohlender, Germany). The outlet of the tube (left side) was furnished with a polyethylene filter. The center tube was connected at both ends via tubing to Teflon/PEEK (wetted parts) 4-port switching valves, bulkhead version (Upchurch Scientific, U.S.A.). One inlet port of the right valve was connected through a peristaltic pump with a flask containing 0.01 M HCl (dissolving solution), the second inlet port was opened through a peristaltic pump to air. One outlet port was connected with the center tube while the second one was plugged. One outlet port of the left switching valve was connected to a membrane pump and the second one lead to vials collecting the desired solution. One inlet port was connected with the center tube and the second one was plugged. An important part of the system were also the tongs used to break the ampoule by bending the center tube and for holding or moving the center tube.

The ampoule to be opened was washed in methanol, water, hot 50% hydrochloric acid and again water, and inserted into the center tube, so that the end containing the activity was on the left hand side. All connections were tightened and the center tube was placed in a vertical position with the left end showing upwards. All ports on the right valve were closed. The system was connected only to the membrane pump through the valve on the left side. The system was evacuated for about 2 min, then the ampoule was broken by depressing the arms of the tongs and the evacuation continued for another 30 s. Then, the ports on the left valve were closed, while the inlet port of the right valve connecting the center tube with acid solution was opened and pumping with the peristaltic pump started. The filling of the center tube containing the broken ampoule with acid solution was accompanied by agitation of the tube with the help of the tongs. The pumping was stopped as soon as the center tube was filled with solution and the agitation continued for few more minutes. Then, the center tube was turned so that the right end was showing upwards, the outlet port on the left valve facing to the vial was opened, and the right valve was

Figure 3.5: Picture of the system for irradiated ampoule breaking. Detailed description in text.

positioned so that the center tube was connected to air. The pumping of air into the system started, in order to push the solution out of the center tube into the collecting vial. When this was finished, the center tube was turned upside down and filled with a new portion of acid solution. The process was repeated (usually three times) to recover a maximum of the activity from the ampoule. When the process was finished, the center tube together with the filter and the cullet was discarded.

Gammaspectrometry

The activity of ^{177}Lu and ^{177m}Lu in the irradiated samples was measured from the unopened ampoules at a distance of 15 cm with a calibrated germanium detector coupled to multichannel analyzer. When the activity of other isotopes was to be determined in the sample (e.g. the long-lived activation impurities), the ampoule with the sample was opened and an aliquot of the obtained solution was measured

in a LSC vial. Decay times were generally so long that the dead time of the detector during counting was $< 1\%$. The obtained γ spectra were analysed with the help of the program MULTINAA [80] using a newly created radionuclide library. The data listed in Tab. 2.2 were employed to evaluate the activity of lutetium isotopes. In general, the most intense γ peak was used to determine the activity of a given isotope. In case that this peak was not free of contributions from other isotopes, another suitable γ peak was chosen. The determination of the ^{177}Lu activity was based on the 208.37 keV peak, while in the case of ^{177m}Lu it was the 228.48 keV peak. It should be noted that ^{177m}Lu contributes to the 208.37 keV peak, but due to its low activity in comparison with the activity of ^{177}Lu, this contribution was neglected. The measurement of the ^{177m}Lu activity in the samples was done as soon as ^{177}Lu was substantially decayed (2-3 months decay time).

Chapter 4

Results and Discussion

4.1 Neutron flux parameters

The new Munich research reactor FRM-II started operation in March 2004 and full power was reached in August 2004 for the first time. The knowledge of its neutron flux parameters is necessary for an accurate calculation of the yield of activation reactions for which the cross section is not reciprocally proportional to the neutron velocity. The activation of ^{176}Lu, which was studied in this work, belongs to such non-$1/v_n$ reactions. The neutron flux is characterized by the following parameters: shape factor of the epithermal flux (α-factor), thermal-to-epithermal neutron flux ratio f, Westcott spectral index $r(\alpha)\sqrt{\frac{T_n}{T_0}}$, thermal neutron flux temperature t_n, thermal-to-fast neutron flux ratio f_{fast}, and thermal ϕ_{th}, epithermal ϕ_{epi}, and fast ϕ_{fast} neutron fluxes.

The neutron flux parameters of the FRM-II reactor were determined by X. Lin two weeks after the reactor reached its full power for the first time [71]. A new determination at the capsule irradiation position KBA 1-1 was conducted within the scope of the present dissertation. The neutron flux parameters were calculated from the activation spectra of flux monitors irradiated in February 2006. The obtained values are given in Tab. 4.1, together with the values obtained by X. Lin in September 2004. The evaluated uncertainties of the determined parameters are large (in the range of tens to hundreds of percent), except for the thermal-to-fast neutron flux ratio, f_{fast}, (uncertainty 5%) and the thermal neutron flux, ϕ_{th}, (uncertainty 4%)

Table 4.1: Neutron flux parameters at the capsule irradiation position KBA 1-1 of FRM-II determined at two different days (21-Feb-06 was the 51^{st} day of the reactor cycle). The data in the second column are taken from [71].

	Irradiation date	
Parameter	11-Sep-04	21-Feb-06
α	0.0567	0.0550
$r(\alpha)\sqrt{\frac{T_n}{T_0}}$	0.00195	0.00193
t_n	11.7	18.9
ϕ_{th}	1.29×10^{14}	1.35×10^{14}
f	457	460
f_{fast}	333	339

[71]. As can be seen in Tab. 4.1, the flux parameters, with the exception of the thermal neutron flux temperature, t_n, remain approximately constant over time. The unexpectedly low temperature of 11.7°C, measured by Lin [71], was in fact found only once at the beginning of the reactor operation and later determinations were roughly in the range of 20–30°C, which is closer to the heavy water temperature in the moderator tank (40–70°C) [71]. The thermal neutron flux was found to be about 4.7% higher than that measured by X. Lin, but this was not surprising as a similar trend was observed previously (discussion later in this section). From the high thermal-to-epithermal neutron flux ratio (f), it can be concluded that the neutrons at the irradiation position KBA 1-1 are highly thermalized and that the contribution of epithermal neutrons to the activation is negligible.

The changes in the value of the thermal neutron flux temperature, t_n, and in the thermal neutron flux, ϕ_{th}, have the largest effect on the calculated ^{177}Lu irradiation yield, whereas the changes of other neutron flux parameters influence the calculated activity to a much lesser extent. On that account, t_n and ϕ_{th} were monitored during several reactor cycles. In Tab. 4.2, the measured values together with average values are listed. The uncertainties of the determined t_n values are large (80–115%), whereas the uncertainties of the thermal neutron flux values are less than 4%, as was determined by X. Lin [71]. It was found that the thermal neutron flux temperature is not stable and varies in the range of $\sim$20–30°C during the reactor cycle. The ther-

Table 4.2: Monitoring of the thermal neutron flux, ϕ_{th}, and the thermal neutron flux temperature, t_n, in KBA 1-1. The reactor operation cycle is 52 days.

Day of reactor operation cycle	Irradiation date	ϕ_{th} $cm^{-2}s^{-1}$	t_n °C
1^{st}	24-May-06	1.27×10^{14}	20.9
2^{nd}	27-Oct-05	1.26×10^{14}	26.2
13^{th}	9-Nov-05	1.29×10^{14}	21.7
26^{th}	19-Jun-06	1.34×10^{14}	23.7
34^{th}	30-Nov-05	1.35×10^{14}	21.0
50^{th}	19-Dec-05	1.42×10^{14}	27.3
52^{nd}	14-Jul-06	1.39×10^{14}	28.0
Average value		$(1.33 \pm 0.06) \times 10^{14}$	24.1 ± 3.0

mal neutron flux seems to show a slight increase during the reactor operation cycle, from $\sim 1.26 \times 10^{14}$ $cm^{-2}s^{-1}$ at the beginning of the cycle to $\sim 1.40 \times 10^{14}$ $cm^{-2}s^{-1}$ at the end of the cycle.

A simultaneous irradiation of two ampoules containing flux monitors at opposite ends of the ampoule was made to evaluate the thermal neutron flux gradient in KBA 1-1. The gradient was found to be $\sim 2.3\%$ for 1-cm distance or 11.3% for 5-cm distance (about the lenght of one ampoule), which can have a considerable influence on the activation yield. The sample to be irradiated is placed at one end of the ampoule and the ampoule can be placed upright or upside down in the irradiation position, thus being exposed to different fluxes. It is not so easy to guarantee every time the same positioning in the irradiation position during routine irradiations because the service staff decides how the packed sample will be placed in the irradiation container.

For the calculation of the $^{176}Lu(n,\gamma)^{177}Lu$ reaction yield, the values of the neutron flux parameters obtained in February 2006 were used (Tab. 4.1), except for t_n and ϕ_{th}, for which the average values given in Tab. 4.2 were used. For other calculations, requiring only the knowledge of ϕ_{th}, the average value from Tab. 4.2 was applied.

4.2 Production of ^{177}Lu

The subject of the present dissertation was the investigation of the direct and the indirect production routes of the therapeutic radionuclide ^{177}Lu at the Munich research reactor FRM-II. In this section, the experience gained and the obtained data are discussed. Suitable target materials, appropriate irradiation positions, and irradiation and decay times are discussed. Further, the design of a system serving to open irradiated ampoules and to dissolve the samples is presented. The experimental irradiation yields of ^{177}Lu for both production routes are evaluated and compared with calculated ones. An estimation of the maximum specific activity obtainable at FRM-II is given. Finally, the content of radionuclidic impurities found in irradiated ^{176}Lu and a discussion of their importance is presented.

4.2.1 Targetry and irradiation

Lutetium-177 was produced by irradiation of ^{176}Lu or ^{176}Yb in the form of nitrates. The nitrate form was evaluated as the most convenient one for two reasons. First, the thermal neutron self-shielding decreases with decreasing atom density of the irradiated material [69], so it is lower for nitrates compared to chlorides or oxides. Second, the nitrates are easily dissolved in diluted hydrochloric acid or even in water, which simplifies the target processing after irradiation.

Commercially available are lutetium and ytterbium oxides of various isotopic enrichment grades. The higher the enrichment of the target isotope, the higher the specific activity and radionuclidic purity of the product. The oxides of highest enrichment currently available on the market were purchased and their isotopic composition determined by ICP-MS. The obtained values are given in Tab. 4.3. When compared with the values given by the distributor (which gives only the enrichment of isotopes with mass number 176), good accordance was found. Only values given by the distributor (Tab. 3.1) were used for calculations.

The target material was sealed in quartz ampoules of dimensions suitable for irradiation and post-irradiation processing. Quartz has a high thermal and radiation stability and minimizes the possibility of sample contamination with metal elements.

Table 4.3: Isotopic composition of purchased enriched lutetium and ytterbium oxides, as analysed by ICP-MS at our institute. If "–" is given, then the data were not available or are not of relevance.

Isotope	Isotope content (%)		
	$^{176}Lu_2O_3$ (64.3%)	$^{176}Lu_2O_3$ (82.2%)	$^{176}Yb_2O_3$ (97.1%)
^{175}Lu	35.65	16.902	–
^{176}Lu	64.35	83.098	–
^{168}Yb	–	–	0.00043
^{170}Yb	–	–	0.02447
^{171}Yb	–	–	0.14769
^{172}Yb	–	–	0.28299
^{173}Yb	–	–	0.29354
^{174}Yb	–	–	2.24414
^{176}Yb	–	–	97.00675

The ampoules used for irradiation have to be robust enough to withstand manipulation and pressure build-up during irradiation, but not too thick-walled to break afterwards. Too small inner diameters of the ampoules hinder the dissolution of the sample due to air bubbles sticking to the inner surfaces, especially at the end where the sample is deposited. Ampoules of 6-mm outer diameter and 0.5-mm wall thickness were found to be optimal.

In case of the direct production route, the irradiation position providing the highest thermal neutron flux is desirable because the specific activity of the product is proportional to the neutron flux. A large component of epithermal neutrons at the irradiation position is also desirable because ^{176}Lu has a strong resonance in the thermal/epithermal neutron area. On the other hand, the value of the neutron flux does not have such a profound effect on the quality of the obtained ^{177}Lu in the case of the indirect production route, but higher flux of course makes the production more effective and the Lu/Yb separation easier. All discussed samples in this work were irradiated in position KBA 1-1, providing highest thermal and epithermal neutron fluxes. Although this position has the highest thermal-to-epithermal neutron flux ratio available at FRM-II [71], the epithermal neutron flux is still very low and the contribution of epithermal neutrons to the irradiation yield is, regrettably, negligible.

4.2.2 Recovery of activated lutetium

To recover the irradiated material in a form suitable for further chemical processing, irradiated ampoules have to be opened and their content dissolved, preferably in a small volume of $\sim 0.05\,\mathrm{M}$ HCl. An ampoule can in principle be opened by two methods. One is the cutting with a rotating diamond saw. However, it was shown that during this operation, some quartz and saw dust enters the ampoule and contaminates the product solution with elements like Ca, Cu, Fe, Mg, Pb, Ni, and Zn, which compete with Lu during labeling of radiopharmaceuticals [13, 43]. The second method is to break the ampoule mechanically by various means.

A system for ampoule breaking and sample dissolution was constructed in the course of the present dissertation. The requirements that were posed on the system included:

- The ampoule should be opened by breaking into several pieces rather than crushed into many small splinters.
- Breaking of the ampoule and dissolution of its content should occur in one closed system so that the contamination of the work place is excluded.
- The dissolving solvent and the product solution should come into contact only with chemically inert materials, the use of metal parts should be avoided.
- The inner volume of the system should be as small as possible so that the product is not unnecessarily diluted (evaporation increases the content of chemical impurities).
- The system set-up should allow switching to full remote control or at least minimizing manual operation and enable control from a safe distance.
- High product recovery is desirable.

The constructed system was described in detail in the experimental section (Sect. 3.2.3). Some of the features of the system will be elucidated here. The ampoules of 0.5-mm wall thickness could be broken easily with the help of tongs, without unnecessary crushing. The evacuation of the system ensured unhindered access of the dissolving solution to all ampoule splinters in the center tube. The employed

4-port switching valves can be mounted to actuators and controlled remotely. The insertion of the ampoule into the center tube is the most critical step (concerning manual work and thus exposure to radiation) and should be done with the help of robotics. Tongs with grips long enough should be used to manipulate the center tube.

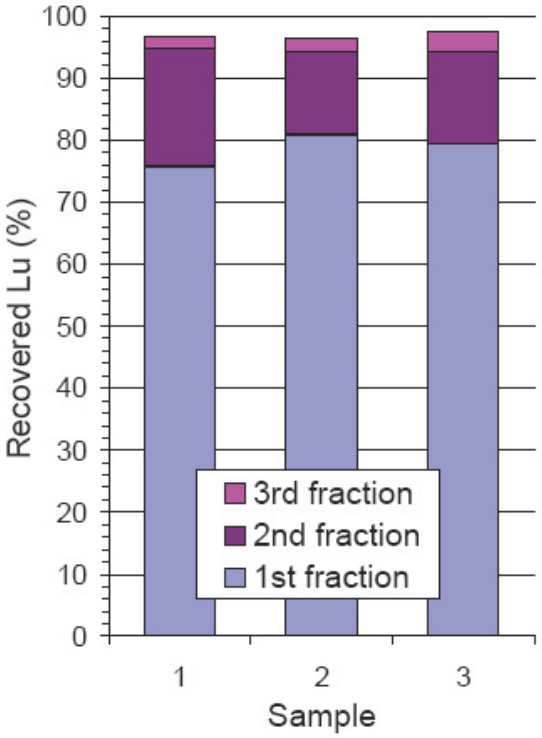

Figure 4.1: Recovery of lutetium from samples irradiated in quartz ampoules using the system for irradiated ampoule breaking. The fractions were obtained by subsequent dissolution and recovery of the ampoule content, as described in the experimental section (Sect. 3.2.3).

The recovery of ^{177}Lu from three irradiated ^{176}Lu$(NO_3)_3$ samples using the designed system is shown in Fig. 4.1. Up to 96–98% of lutetium dissolved in $\lesssim$5.4 mL of 0.01 M HCl was obtained in three fractions. The purity of the obtained ^{177}Lu preparations was analysed with ICP-OES. The most important chemical impurities found in the first fractions of samples # 2 and # 3 are given in Tab. 4.4. Calcium, iron, nickel, and zinc, all being strong competitors for lutetium during the labeling of radiopharmaceuticals, were found in the recovered lutetium solutions, but at low concentrations. The total concentration of chemical impurities in the lutetium frac-

Table 4.4: Chemical impurities found in lutetium fractions recovered using the system for breaking of irradiated ampoules. Values in the second column are given for reference and represent the composition of a lutetium preparation obtained at the Radioisotope Centre POLATOM, Poland [43] by breaking the irradiated quartz ampoule mechanically. Values given in the last two columns were obtained by ICP-OES analysis of the first fractions of opened samples # 2 and # 3 (see Fig. 4.1). If "<d.l." is given, then the concentration was lower than the detection limit. If "–" is given, then the concentration of the element was not measured.

Element	Concentration (ng/g)		
	POLATOM	sample 2	sample 3
Al	6280	74	–
Ca	835	167	69
Cu	15	226	<d.l.
Cr	197	<3	–
Fe	126	500	275
Mg	–	5	6
Ni	45	334	209
Pb	30	<5	<d.l.
Zn	114	39	38

tions obtained using the system for breaking of irradiated ampoules is not expected to exceed few ppm, which should be acceptable for the preparation of radiopharmaceuticals.

4.2.3 Yield of the ^{176}Lu (n, γ) ^{177}Lu reaction

When calculating the ^{177}Lu activity produced in the ^{176}Lu (n, γ) ^{177}Lu reaction, two significant effects have to be taken into account. The high cross section of ^{176}Lu for thermal neutron capture causes intensive target burn-up, so that the number of target atoms cannot be considered to be constant during irradiation. Further, the cross section of the reaction has a strong resonance at 0.1413 eV (see Fig. 2.3(a)), so that the $\sigma(v_n)$ function deviates from the $1/v_n$ law. In such cases, the Westcott convention

has to be used for the calculation of the reaction rate. Thus the combination of Eqs. 3.8 and 3.12 gives for the activity of produced ^{177}Lu:

$$A = \frac{\lambda N \phi_{th} \sigma_0 k}{\lambda - \phi_{th} \sigma_0 k} (e^{-\phi_{th} \sigma_0 k t} - e^{-\lambda t}), \tag{4.1}$$

where k is so called k-factor, given by:

$$k = [G_{th} \cdot g(T_n) + G_r \cdot r(\alpha) \sqrt{\frac{T_n}{T_0}} \cdot s_0(\alpha)], \tag{4.2}$$

and λ is the decay constant of ^{177}Lu, N is the initial number of ^{176}Lu atoms in the target, and σ_0 is the neutron capture cross section of ^{176}Lu at the neutron velocity of 2200 $\mathrm{m \cdot s^{-1}}$. In the calculation, the self-shielding factors were set equal to 1, the constants s_0 and $\bar{E}_r$ were equal to 1.67 and 0.158 eV, respectively [78]. The Westcott factor was derived from the measured neutron temperature (Tab. 4.2) using the data published in [81]. All other data were taken from Tabs. 2.2, 4.1, and 4.2.

The value of the k-factor calculated for the position KBA 1-1 of the Munich reactor is equal to ~ 1.78. Figure 4.2 shows the calculated variation of the k-factor with neutron temperature, t_n. As can be seen, the dependence is almost linear, with k-factors ranging from 1.75 at 20°C to 2.12 at 70°C.

The theoretical dependence of the irradiation yield of the $^{176}\mathrm{Lu}(n,\gamma)^{177}\mathrm{Lu}$ reaction on irradiation time, calculated using Eq. 4.1, is presented in Fig. 4.3. Further, the irradiation yield calculated using Eq. 3.8, which is identical with Eq. 4.1 when the k-factor is set equal to 1, is shown in Fig. 4.3. This second calculation represents the common but incorrect way to compute the ^{177}Lu yield, as will be illustrated later. According to theoretical predictions, the activity of ^{177}Lu formed in the irradiated lutetium target is increasing linearly during the first several hours of the irradiation. Later the burn-up of the target material becomes evident and the irradiation yield reaches a maximum. The time of irradiation providing the maximum ^{177}Lu activity can be found when the differentiation of Eq. 4.1 with respect to irradiation time is set equal to zero. The so called t_{max} can then be calculated as:

$$t_{max} = \frac{1}{\lambda - \phi_{th} \sigma_0 k} \ln \frac{\lambda}{\phi_{th} \sigma_0 k}, \tag{4.3}$$

from where it becomes evident that the irradiation time necessary for reaching max-

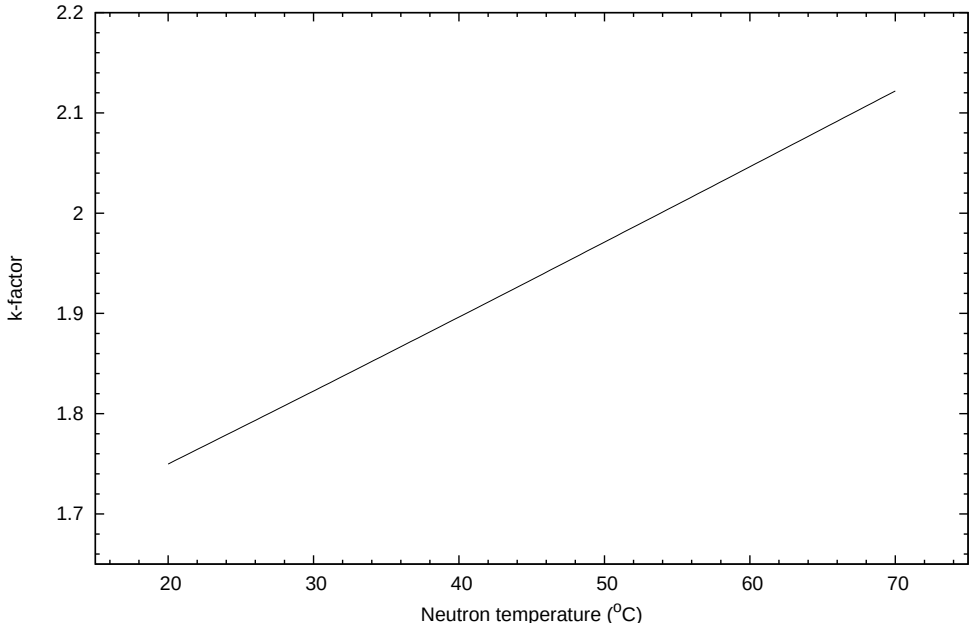

Figure 4.2: The dependence of the k-factor, calculated using Eq. (4.2), on thermal neutron flux temperature, t_n. Calculated for position KBA 1-1, FRM-II.

imum ^{177}Lu activity in the system is decreasing with increasing neutron flux and k-factor. The t_{max} calculated for the irradiation position KBA 1-1 at FRM-II is equal to 14.7 days.

Activities of ^{177}Lu measured in the irradiated ^{176}Lu$(NO_3)_3$ targets together with theoretically calculated values are presented in Fig. 4.4. It is obvious at first glance that the calculation based on the modified Westcott convention fits the experimental data much better than the calculation usually employed. The average ratio of the experimental ^{177}Lu yield and the yield calculated using the modified Westcott convention was found to be 1.03 ± 0.03 for Lu with 64.3% enrichment and 1.09 ± 0.04 for Lu with 82.2% enrichment. The measured ^{177}Lu activity was in the majority of the cases higher than the calculated one. The difference in the case of lutetium with 82.2% enrichment is 9% on average, which is more than the estimated experimental error (less than 5%). The difference is probably due to more than one reason. The most important ones are probably: (a) The error in the thermal neutron capture cross section of ^{176}Lu (values of 2020 ± 70 b or 2090 ± 70 b are given in the literature [28, 82]). (b) The error in the determination of the neutron flux parameters. (c) The

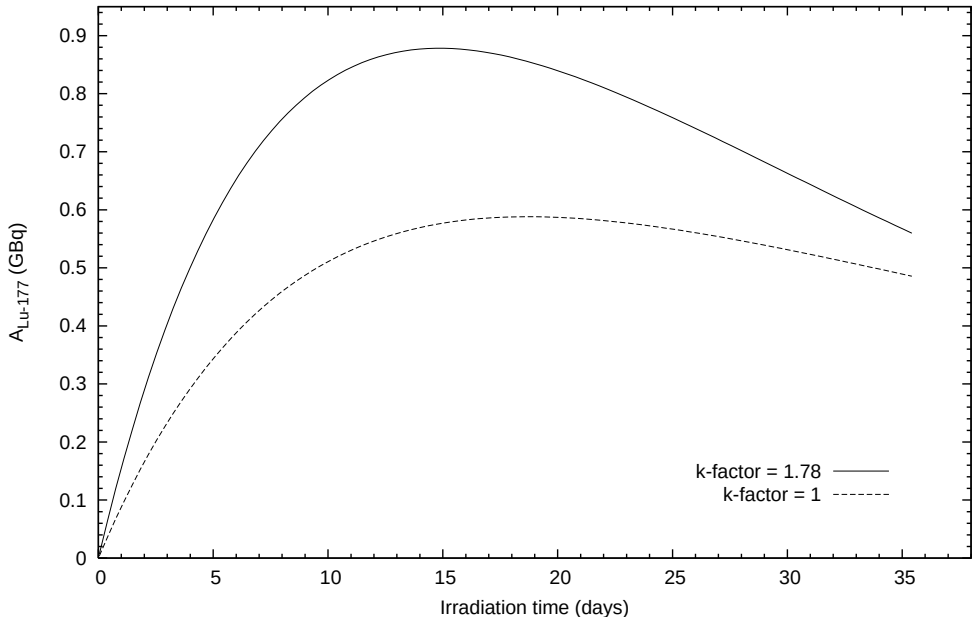

Figure 4.3: Irradiation yield of the ^{176}Lu (n, γ) ^{177}Lu reaction calculated using the modified Westcott convention with a k-factor equal to 1.78 (irradiation position KBA 1-1 of FRM-II) or with a k-factor equal to 1 (the common way of calculation) for a target containing 1 μg of ^{176}Lu and a thermal neutron flux of 1.3×10^{14} cm^{-2}s^{-1}.

error of the ^{176}Lu mass in the target, caused by higher enrichment or an inaccurate lutetium stock solution concentration. The last reason is probably responsible for a large part of the error in the case of Lu with 82.2% enrichment. To find the answer, more experiments would be needed.

Nevertheless, the calculation based on the modified Westcott convention has proved to be sufficiently precise for the purposes of ^{177}Lu production. It provides a reliable tool for the prediction of the ^{177}Lu irradiation yield, under the condition that the neutron flux parameters at the irradiation position are known. For comparison, the discrepancies between predicted and experimentally determined lutetium activities after ^{176}Lu activation given in the literature are in the range of 14–100 % [39, 42, 45, 46].

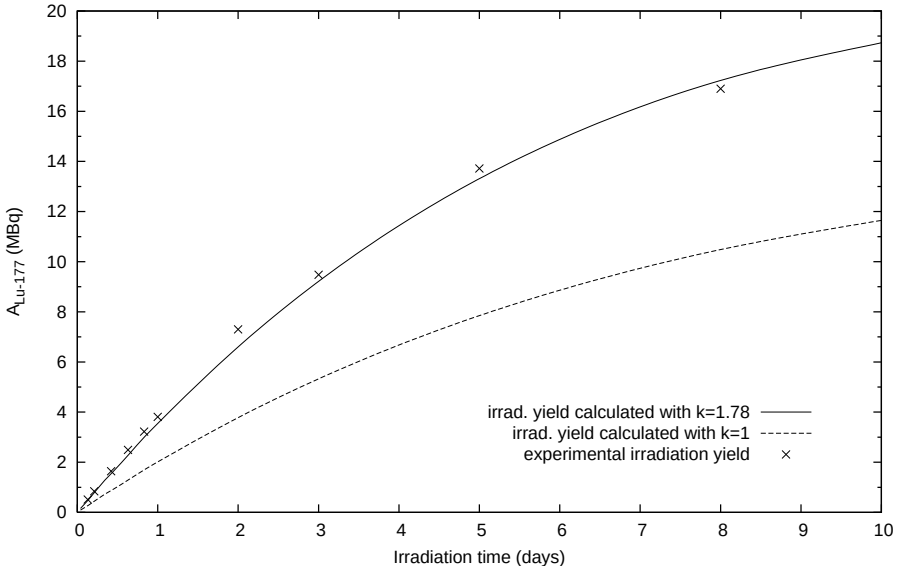

(a) Targets with 64.3% isotopic enrichment.

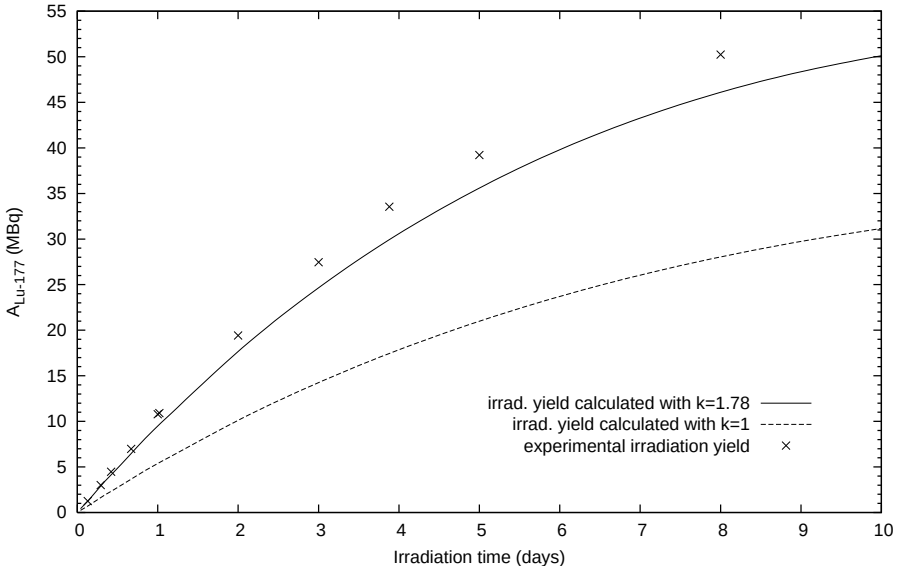

(b) Targets with 82.2% isotopic enrichment.

Figure 4.4: Comparison of the irradiation yield calculated using the modified Westcott convention (Eq. 4.1) or calculated in the common way (Eq. 3.8) and experimentally determined activity of ^{177}Lu in ^{176}Lu$(NO_3)_3$ targets with 64.3% or 82.2% isotopic enrichment. The given experimental irradiation yield is always an average of the lutetium activity in three targets irradiated together. The estimated error of the experimental data is less than 5%.

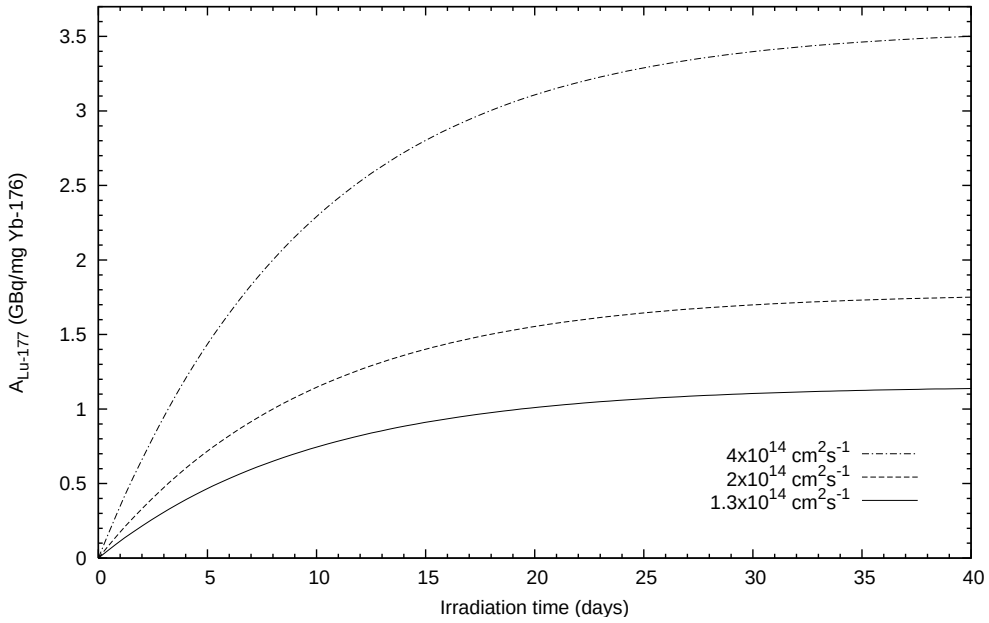

Figure 4.5: The activity of ^{177}Lu produced in the ^{176}Yb (n,γ) ^{177}Yb $\overset{\beta^-}{\rightarrow}$ ^{177}Lu reaction calculated using Eq. 4.4 with 24 hours post-irradiation decay period and three different thermal neutron fluxes.

4.2.4 Yield of the ^{176}Yb (n,γ) ^{177}Yb $\overset{\beta^-}{\rightarrow}$ ^{177}Lu reaction

The target burn-up is negligible in the case of the ^{176}Yb (n,γ) ^{177}Yb reaction and the cross section follows the $1/v_n$ law (see Fig. 2.4). The ^{177}Lu activity produced in the ^{176}Yb (n,γ) ^{177}Yb $\overset{\beta^-}{\rightarrow}$ ^{177}Lu reaction can thus be calculated using the following equation (cf. Eq. 3.13):

$$A = \lambda_Z N_X \phi_{th} \sigma_X \left[\left(\frac{1 - e^{-\lambda_Z t}}{\lambda_Z} + \frac{e^{-\lambda_Y t} - e^{-\lambda_Z t}}{\lambda_Y - \lambda_Z} \right) e^{-\lambda_Z t_d} + \frac{(1 - e^{-\lambda_Y t})(e^{-\lambda_Y t_d} - e^{-\lambda_Z t_d})}{\lambda_Z - \lambda_Y} \right] \tag{4.4}$$

where index X stands for ^{176}Yb, Y for ^{177}Yb, and Z for ^{177}Lu.

The activity of ^{177}Lu calculated using Eq. 4.4 with 24 hours post-irradiation decay period is shown in Fig. 4.5. The activity increases monotonously with irradiation time up to the saturation value, A_{sat}, given by the product of the ^{176}Yb cross section,

thermal neutron flux, and the number of ^{176}Yb target atoms. An irradiation of 5 days provides 40% of A_{sat}, while a 10-day irradiation provides 64% of A_{sat} and a 15-day irradiation 79% of the ^{177}Lu saturation activity. Lutetium-177 is formed during the irradiation but also for some period after the end of the irradiation by the decay of ^{177}Yb with a half life of 1.9 h. This post-irradiation contribution to the total ^{177}Lu activity decreases sharply with irradiation time (see Fig. 4.6) and becomes negligible (<4%) for irradiation times longer than 5 days.

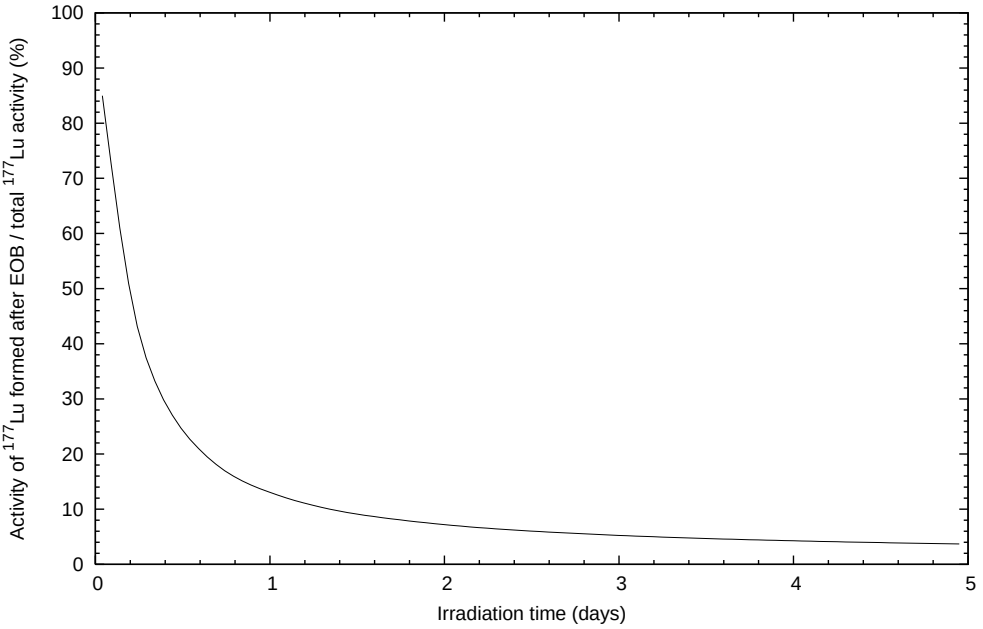

Figure 4.6: The post-irradiation contribution to the total ^{177}Lu activity from the decay of ^{177}Yb produced in the ^{176}Yb (n,γ) ^{177}Yb reaction calculated as a function of the irradiation time.

Activities of ^{177}Lu measured in irradiated ^{176}Yb$(NO_3)_3$ targets together with values theoretically calculated using Eq. 4.4 are presented in Fig. 4.7. The experimental values were found to be about 10% lower than the theoretical ones ($A_{exp}/A_{teor} = 0.91 \pm 0.02$). That could be explained most probably by the error in the thermal neutron cross section of ^{176}Yb used in the calculations because the cross sections given by approved sources vary considerably: 2.4 ± 0.2 b [83], 2.85 ± 0.05 b [28], and 3.1 b [27]. When an effective cross section of 2.6 b (determined in this work) is used in the calculations, then Eq. 4.4 provides a very accurate way of predicting the ^{177}Lu yield in the indirect production route ($A_{exp}/A_{teor} = 0.99 \pm 0.02$). A different experimental

yield of ^{177}Lu in the indirect production route compared to the theoretical one was reported also by Knapp et al. [39] (20% lower exp. yield using 2.85 b cross section) and by Mikolajczak et al. [42] (10–25% lower exp. yield for natural Yb and 10–25% higher exp. yield for enriched Yb using 2.4 b cross section).

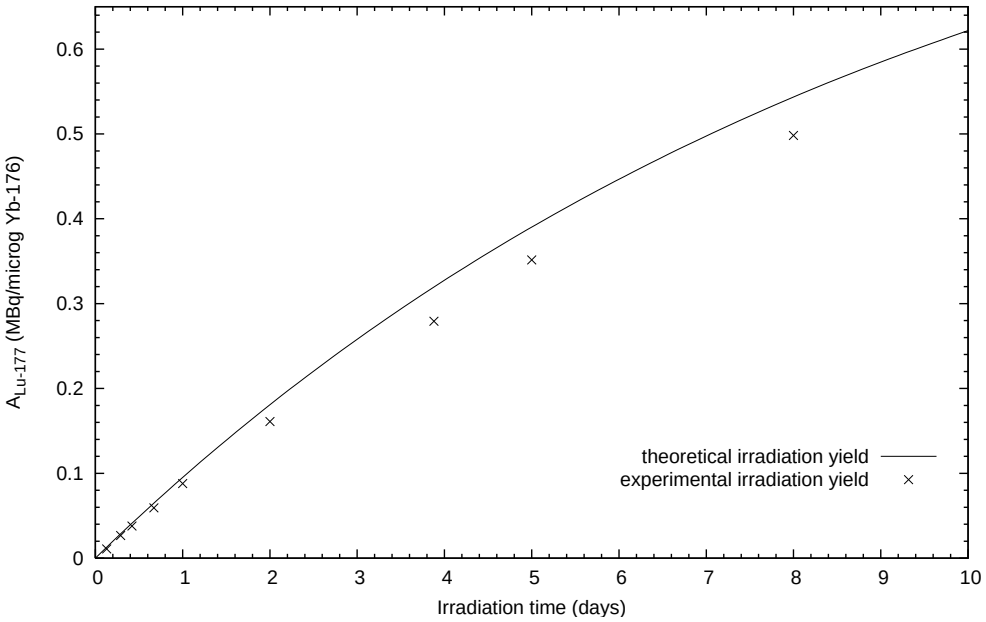

Figure 4.7: Comparison of the calculated ^{177}Lu activity (Eq. 4.4) and the experimentally determined yield of the ^{176}Yb (n,γ) ^{177}Yb $\xrightarrow{\beta^-}$ ^{177}Lu reaction (with 72 hours post-irradiation decay period). Targets of ^{176}Yb$(NO_3)_3$ with 97.1% isotopic enrichment were irradiated in position KBA 1-1 of FRM-II (thermal neutron flux of 1.33×10^{14} cm^{-2}s^{-1}). The given experimental irradiation yield is always the average of the lutetium activity in three targets irradiated together. The estimated error of the experimental data is less than 5%.

4.2.5 Specific activity

It was already mentioned in the introductory chapter that the specific activity of a radionuclide is a very important quantity determining its applicability in nuclear medicine. Radionuclides of very high specific activity are required for some applications. A radionuclide has a maximum specific activity when it is the only isotope of the element present in the system. If ^{177}Lu is the only isotope of lutetium present,

then its specific activity is equal to 4100 GBq/mg or 111 Ci/mg. Lutetium-177 with specific activities higher than $\sim$15–20 Ci/mg (555–740 GBq/mg) is currently required for peptide receptor radionuclide therapy [13, 84].

When the radionuclide is produced by the (n, γ) reaction in a nuclear reactor, then its specific activity is usually related to the initial mass of the respective element in the target, because the produced radionuclide is an isotope of the target element. If the burn-up of the target can be neglected, then the calculated specific activity agrees well with the real value. However, if the cross section of the reaction is so high that the target element is used up during the irradiation, then the specific activity should be related to the actual mass of the respective element. This rule has an exception in the case of radiolanthanides, which decay into neighboring lanthanides competing with the original element during the labeling of radiopharmaceuticals, so that the specific activity is related to the total mass of all lanthanides.

Lutetium-176 has the highest thermal neutron capture cross section found among the lanthanides and the activation product ^{177}Lu(III) decays into the stable ^{177}Hf(IV), which does not compete with ^{177}Lu during the labeling of radiopharmaceuticals, as was shown by [13]. Figure 4.8 shows the mass distribution of lutetium isotopes in the target at any time during the irradiation (for position KBA 1-1, FRM-II). The mass of ^{175}Lu is not shown in the graph because its change is $<$ -0.5% after 2 weeks of irradiation. On the other hand, the burn-up of ^{176}Lu cannot be neglected. As can be seen in Fig. 4.8, the total mass of lutetium isotopes (175, 176, 177) in the target is decreasing during the irradiation, being $\sim$20% lower at the moment when the ^{177}Lu activity reaches a maximum than at the start of irradiation.

The changes of the ^{177}Lu specific activity during the irradiation are presented in Fig. 4.9. Two calculations are shown - one relates the specific activity to the actual lutetium mass in the target and the second one to the initial target mass (1 mg of enriched lutetium). The dashed line represents at the same time the absolute activity of ^{177}Lu. It is obvious that the maximum specific activity is reached much later than the maximum absolute activity, due to intensive target burn-up. Irradiation for 14.7 days provides 19.7 Ci of ^{177}Lu with a specific activity of 24.5 Ci/mg, while irradiation for 25 days provides 17.0 Ci of ^{177}Lu with a specific activity of 27.2 Ci/mg (calculated for irradiation position KBA 1-1, FRM-II). The optimal irradiation time must be chosen with respect to the required minimum specific activity and the economic

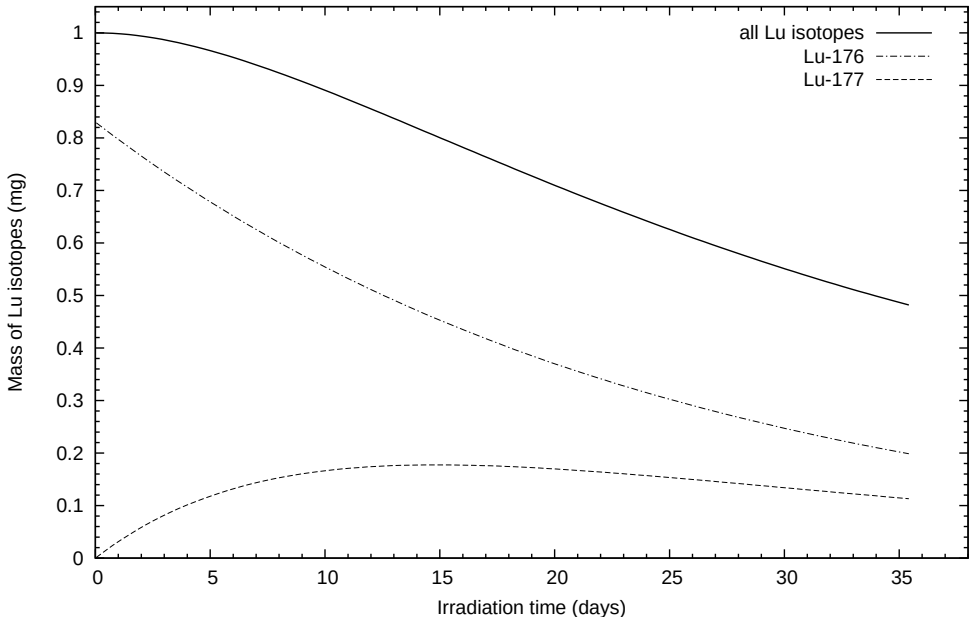

Figure 4.8: Calculated mass distribution of lutetium isotopes in a 1-mg enriched lutetium target (83% of ^{176}Lu) at any time during the irradiation in position KBA 1-1, FRM-II. The curve "all Lu isotopes" comprises isotopes 175, 176, and 177.

expediency of a longer irradiation.

Figure 4.10 illustrates the influence of the thermal neutron flux and the ^{176}Lu enrichment on the specific activity of ^{177}Lu produced in the direct production route. It is evident that the maximum specific activity is achieved much earlier with higher flux and is very high even with lower enrichment. Further, the calculation shows that the increase in the specific activity by irradiation of lutetium with higher enrichment is not so pronounced at low and moderate thermal neutron fluxes.

The situation is very different in the case of the indirect production route, where virtually *n.c.a.* ^{177}Lu is produced. The theoretical specific activity can be, however, obtained only in the ideal case, when monoisotopic ^{176}Yb is irradiated and then completely separated from the produced ^{177}Lu. In practice, the maximum achievable specific activity is lower due to three reasons:

- The ytterbium target always contains some stable lutetium impurity (up to thousands of ppm).

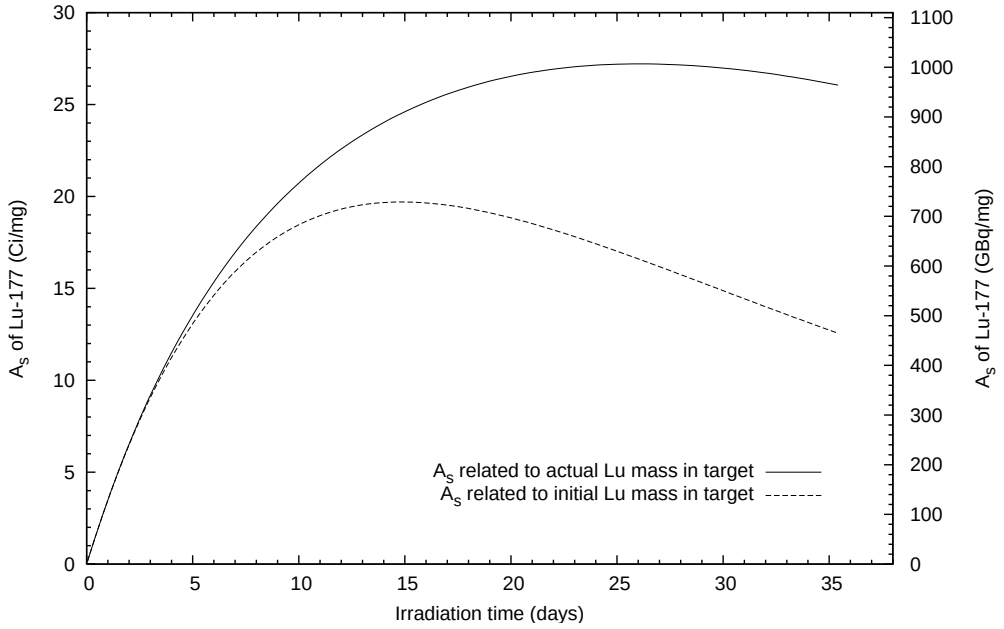

Figure 4.9: Change of the ^{177}Lu specific activity, A_s, during irradiation calculated for a 1-mg lutetium (83% enr.) target irradiated in position KBA 1-1 of FRM-II, related to initial or actual lutetium mass in the target.

- The target is not monoisotopic. It typically contains few percent of ^{174}Yb which causes the production of stable ^{175}Lu in the system via the ^{174}Yb (n,γ) ^{175}Yb $\xrightarrow{\beta^-}$ ^{175}Lu reaction. This contribution to the total lutetium mass in the system is significant due to the relatively high content of ^{174}Yb in the target, the high thermal neutron capture cross section of ^{174}Yb, and shorter half-life of ^{175}Yb compared to ^{177}Lu (for constants see Tab. 2.2). It is advisable to separate ^{177}Lu from the Yb target as soon as possible after the end of bombardment (EOB), because ^{175}Lu is formed by the decay of ^{175}Yb also after the EOB, lowering the specific activity.

- Some amounts of ytterbium always remain in the system after the Lu/Yb separation. Ytterbium competes with lutetium during the labeling of radiopharmaceuticals, so the specific activity has to be related to the total mass of lutetium and ytterbium (in fact to the total mass of all lathanides) in the system.

The effective separation of ^{177}Lu from the ytterbium target is one of the key steps

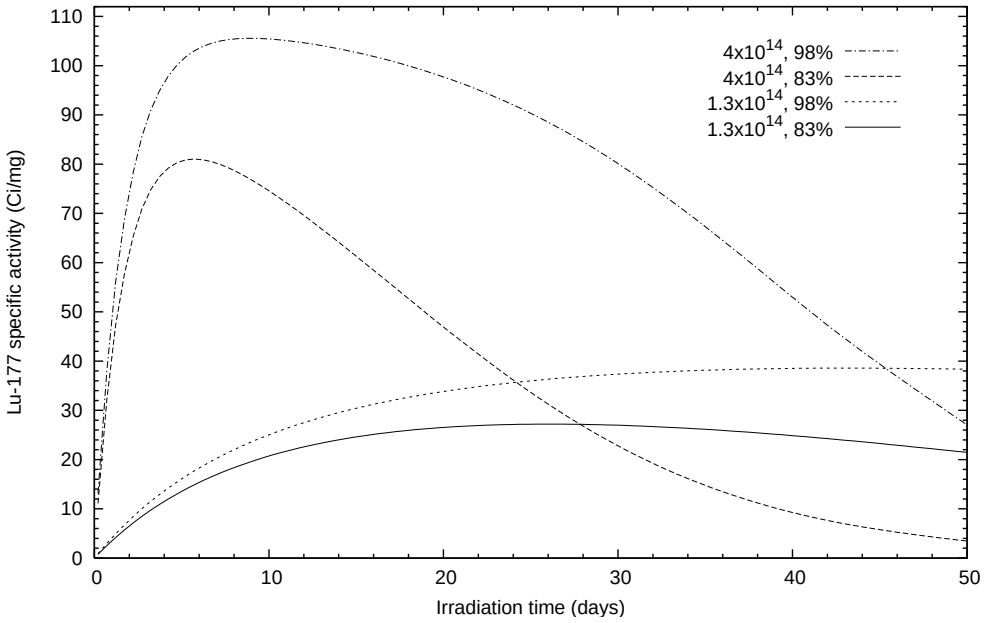

Figure 4.10: Variation of the ^{177}Lu specific activity (related to actual lutetium mass in the target) during irradiation calculated for two different thermal neutron fluxes ($cm^{-2}s^{-1}$) and ^{176}Lu enrichments - see legend. The maximum theoretical specific activity of ^{177}Lu is 111 Ci/mg.

determining the quality (specific activity and radionuclidic purity) of the produced ^{177}Lu preparation. The ytterbium remaining in the system after the Lu/Yb separation should not exceed tens of nanogram because lutetium is present in very low quantities (1 Ci of ^{177}Lu corresponds to the mass of only 9 μg). Figure 4.11 shows the variation of the ytterbium target mass necessary to obtain 1 Ci of ^{177}Lu versus irradiation time. The Yb/Lu mass ratio in the target is one of the properties determining the successful application of the selected separation method. The lower the Yb/Lu mass ratio, the more feasible the separation. For the conditions at the Munich reactor, targets containing not less than 50 mg of enriched ytterbium (97%) have to be irradiated to produce 1 Ci of ^{177}Lu in a 10-day irradiation.

4.2.6 Radionuclidic purity

Radionuclidic purity is one of the closely monitored characteristics of the medical radionuclide preparation. Unwanted radionuclides are produced by activation of

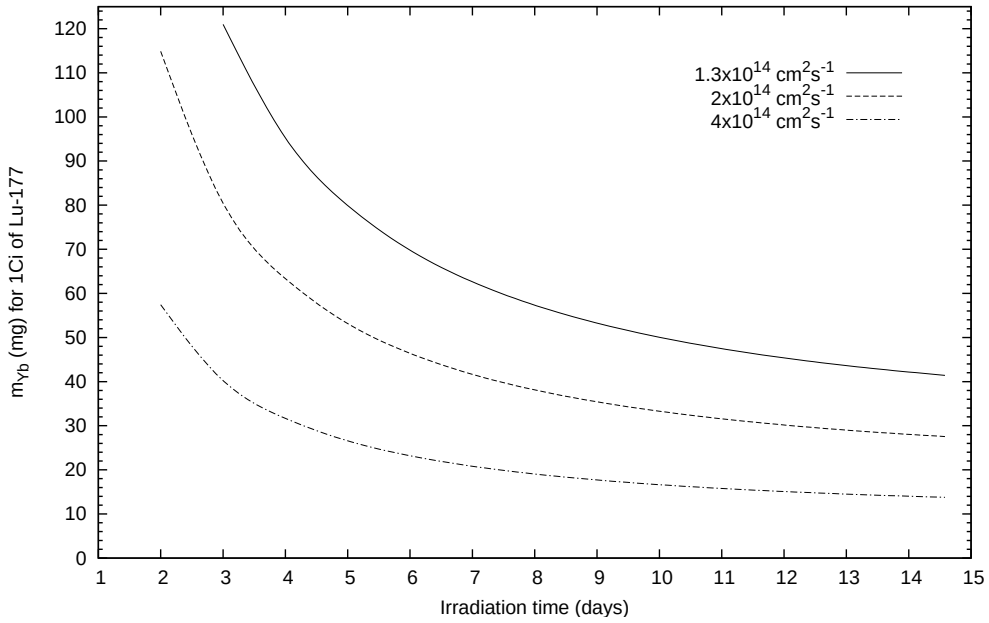

Figure 4.11: The mass of Yb target (97% enrichment) necessary for the production of 1 Ci of ^{177}Lu present in the target 24 hours after EOB calculated for three different thermal neutron fluxes.

chemical impurities present in the target material or by side reactions on the target isotope (not so common in irradiations with thermal neutrons in nuclear reactors). They can also be introduced into the product during the post-irradiation processing. Radionuclidic impurities with half-lives of the order of several days constitute an unnecessary radiation burden for the patient. Long-lived radionuclides (half-life in the range of months to years) are problematic especially with respect to waste disposal at hospitals where a large number of treatments are conducted.

Content of ^{177m}Lu

The long-lived (160.5 days) isomer of ^{177}Lu is inevitably produced in the ^{176}Lu (n,γ) ^{177m}Lu reaction during the direct production of ^{177}Lu. When calculating the ^{177m}Lu activity produced, the same effects have to be taken into account as in the case of the ^{176}Lu (n,γ) ^{177}Lu reaction. The cross section of the former reaction is quite low (2.8 b) but the target is yet burned-up by the parallel (n,γ) reaction leading to ^{177}Lu. The cross section of the reaction has again a strong resonance in the thermal

neutron range (see Fig. 2.3(b)), so that the Westcott convention has to be used for the calculation of the reaction rate. Considering the two (n,γ) reactions, then the net rate of ^{177m}Lu growth can be written as:

$$\frac{\mathrm{d}N_Y}{\mathrm{d}t} = \phi_{th}\sigma_2 k_2 N e^{-\phi_{th}\sigma_1 k_1 t} - N_Y\lambda_Y \tag{4.5}$$

where N is the initial number of ^{176}Lu atoms in the target, N_Y is the number of ^{177m}Lu atoms, σ_1 is the cross section of the ^{176}Lu (n,γ) ^{177}Lu reaction, σ_2 is the cross section of the ^{176}Lu (n,γ) ^{177m}Lu reaction, λ_Y is the decay constant of ^{177m}Lu, and k_1 and k_2 are the respective k-factors. The decay of ^{177m}Lu can be neglected due to its relatively long half-life and the integration of Eq. 4.5 gives:

$$N_Y = \frac{N\sigma_2 k_2}{\sigma_1 k_1}(1 - e^{-\phi_{th}\sigma_1 k_1 t}). \tag{4.6}$$

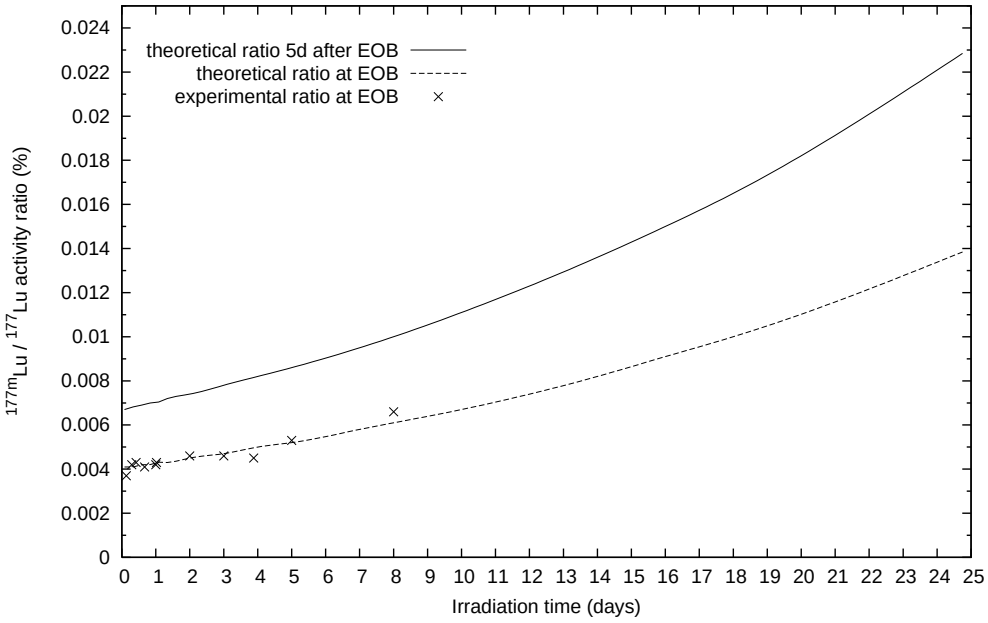

Figure 4.12: The ratio of ^{177m}Lu and ^{177}Lu activities found in irradiated lutetium samples (82.2% enrichment) compared with values calculated using Eq. 4.6 for EOB and with 5 days decay period after EOB.

The k_2-factor can, unfortunately, not be calculated because the necessary constants are not known. Based on experimental data, the k_2-factor in this work was set equal to 1.25 for the purpose of the calculations. Figure 4.12 shows the calculated

^{177m}Lu/^{177}Lu activity ratio at EOB using Eqs. 4.1 and 4.6, and the activity ratios experimentally found in the irradiated ^{176}Lu targets. The relative content of ^{177m}Lu in the lutetium target increases with irradiation time and further grows after the EOB due to the longer half-life of ^{177m}Lu in comparison to ^{177}Lu. Figure 4.12 also shows how the ^{177m}Lu/^{177}Lu activity ratio increases 5 days after the EOB. The calculation with a k-factor of 1.25 seems to fit the experimental data well, however, 15–20 day irradiations should be performed to verify if this holds also at longer irradiation times. The content of ^{177m}Lu found in the lutetium targets (82.2% enrichment) irradiated for 8 days in the position KBA 1-1 of the Munich reactor was $\sim$3450 Bq per 50.6 MBq of ^{177}Lu, resulting in a ratio of 0.0068% at EOB. The expected activity ratio for 15 days of irradiation is $<$ 0.009% at EOB, changing to $<$ 0.015% 5 days after EOB. The values given in the literature are typically $<$ 0.01–0.02% at EOB [39, 43, 45]. The content of ^{177m}Lu in the product is independent of target enrichment. To keep it low, short irradiation and decay times are necessary, which means that ^{177}Lu produced in high-flux reactors has the lowest content of ^{177m}Lu.

A ^{177}Lu preparation produced by the indirect production route does not contain the ^{177m}Lu impurity, making the indirect route in this respect advantageous over the direct one.

Content of other activation impurities

Equation 3.4 was employed to estimate which impurities present in the raw lutetium oxide are critical with respect to their activation during irradiation. Most critical impurities are those having high abundance of isotopes with high thermal neutron capture cross section and half-lives in the range of several days (thus comparable to ^{177}Lu). Radionuclides with much longer half-life are also important because they increase the volume of radioactive waste, which has to be stored or disposed appropriately. Table 4.5 shows the calculation of the yield for impurities whose activation products are expected to have an activity at EOB higher than or close to 10^{-5}% of the activity of ^{177}Lu. The calculation was carried out for 1-μg of enriched lutetium oxide target irradiated in the position KBA 1-1 of FRM-II for 10 days. The last column of the table gives the radionuclide impurity/^{177}Lu activity ratio 3 days after EOB. It is not expected that ^{177}Lu would be used before expiry of this decay period. It should be kept in mind by the evaluation of the "criticality" of the impurities that

Table 4.5: Calculated (using Eq. 3.4) activation of relevant impurities present in 1 μg of lutetium oxide irradiated in KBA 1-1 position of FRM-II for 10 days. The content of impurities in lutetium oxide (82.2% enr.) is given in Tab. 3.1

Elem. impurity	Abund. of parent isotope	Cross section, barn	Activation product	$T_{1/2}$, days	A at EOB, Bq	A/A_{177Lu} at EOB, %	A/A_{177Lu} 3 days decay, %
Mn	1	13.3	^{56}Mn	0.11	271	4.5×10^{-5}	2.9×10^{-12}
Cu	0.69	4.5	^{64}Cu	0.53	63	1.0×10^{-5}	3.3×10^{-6}
La	1	9.0	^{140}La	1.7	362	6.0×10^{-5}	2.4×10^{-5}
Sm	0.27	206	^{153}Sm	1.9	85	1.4×10^{-5}	6.6×10^{-6}
Eu	0.48	3150	^{152m}Eu	0.39	5555	9.2×10^{-4}	5.9×10^{-6}
Dy	0.28	1000	^{165}Dy	0.1	278	4.6×10^{-5}	3.8×10^{-14}
Yb	0.32	100	^{175}Yb	4.2	59	9.9×10^{-6}	8.2×10^{-6}
Lu	0.18	16.7	^{176m}Lu	0.15	1.1×10^{6}	1.9×10^{-1}	3.3×10^{-7}
	0.82	2.8	^{177m}Lu	160	3.9×10^{4}	6.5×10^{-3}	8.8×10^{-3}

$\sim$40 kBq of ^{177m}Lu is produced in the discussed example, representing the main radionuclidic impurity. Radionuclides with much lower irradiation yield than ^{177m}Lu can be disregarded.

It is obvious from Tab. 4.5 that from the considered activation products ^{56}Mn, ^{165}Dy, and ^{176m}Lu decay quickly, being eventually no longer relevant. The content of La, Eu, Sm, and Yb in the raw material should be kept as low as possible because ^{140}La, ^{152m}Eu, ^{153}Sm, and ^{175}Yb with half-lives in the range of 0.4–4.2 days are expected to be produced in small quantities. Nevertheless, even if the content of these elements in the original oxide would be in the range of hundreds of ppm, the activity of the produced radionuclides could be neglected. The calculation also showed that no long-lived radionuclidic impurities, except for ^{177m}Lu, are expected to be found in the irradiated lutetium.

To verify the conclusions based on calculations, lutetium samples irradiated for 8 days were analyzed for the content of long-lived radionuclidic impurities by γ-spectrometry after the decay of ^{177}Lu (2–3 months decay time). No relevant radionu-

clidic impurities except for ^{177m}Lu were found in the samples. The only other radionuclides beside ^{177m}Lu and ^{177}Lu which were observed in the spectrum in very small amounts were ^{169}Yb (1.3×10^{-4}% of ^{177}Lu activity at EOB) and ^{65}Zn (1.8×10^{-4}% of ^{177}Lu activity at EOB). Apart from that, γ peaks of naturally occuring ^{214}Bi (^{238}U decay chain) and ^{40}K (natural K) were also observed. The γ-spectrum of the 8-day sample recorded 3 weeks after the EOB is shown in Fig. 4.13. No peaks except those of ^{177}Lu can be seen due to the high activity of ^{177}Lu. Figures 4.14 and 4.15 show the spectrum of the same sample recorded 3 months after the EOB when esentially all ^{177}Lu originally present has decayed. A great number of ^{177m}Lu γ lines are observed in the range of 100–500 keV. Further, peaks of ^{169}Yb, ^{65}Zn, ^{214}Bi and ^{40}K are observed.

4.2.7 Summary

Two routes, the direct and the indirect one, were investigated for the production of ^{177}Lu at the Munich research reactor FRM-II. Targets of ^{176}Lu$(NO_3)_3$ (direct production route) or ^{176}Yb$(NO_3)_3$ (indirect production route) sealed in quartz ampoules were irradiated for up to 8 days in KBA 1-1, the capsule irradiation facility providing the highest thermal neutron flux available at FRM-II. The activity of ^{177}Lu in the irradiated samples was measured by γ-spectrometry mainly from unopened ampoules. The ampoules were opened and samples dissolved before the determination of activation impurities using a specially constructed system for breaking of irradiated ampoules and sample dissolution. Up to 98% of the produced ^{177}Lu could be recovered in < 5.5 mL of 0.01 M HCl using this system.

The modified Westcott convention was employed for the calculation of the irradiation yield of ^{177}Lu in the direct route. The average ratio of experimental to theoretical ^{177}Lu yields was found to be 1.03 ± 0.03 for lutetium targets with 64.3% enrichment and 1.09 ± 0.04 for lutetium targets with 82.2% enrichment. The effective cross section of the ^{176}Lu (n, γ) ^{177}Lu reaction determined in this work is $\approx$ 3700 b for KBA 1-1. According to calculations, the ^{177}Lu irradiation yield shows a maximum at 14.7 days of irradiation in KBA 1-1. The specific activity of ^{177}Lu (83% enr.) at this point of time is 24.5 Ci/mg. Longer irradiation provides higher specific activity (maximum at 25 days is 27.2 Ci/mg) but the absolute yield of ^{177}Lu is lower.

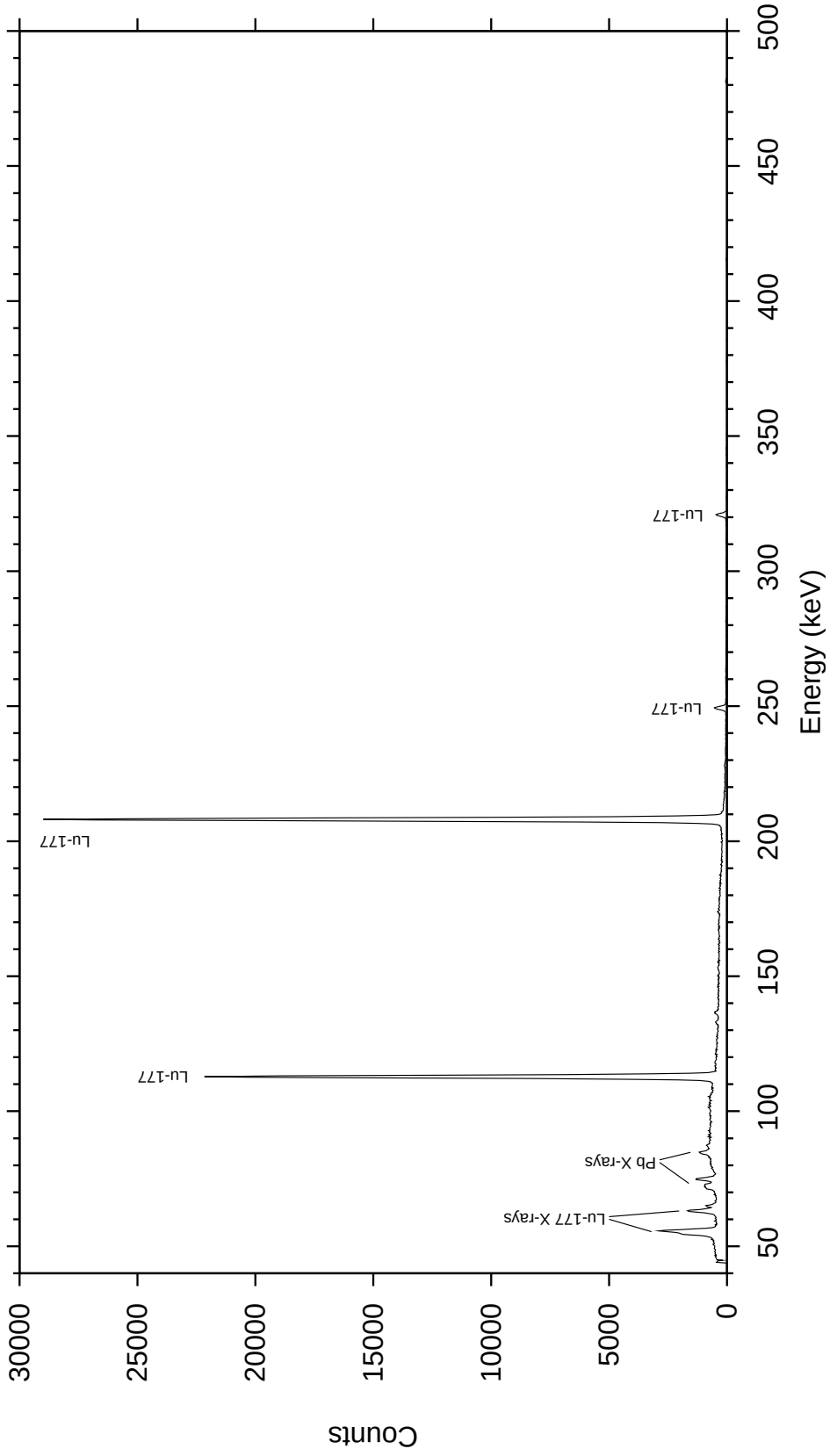

Figure 4.13: Gamma-ray spectrum of a ^{176}Lu target irradiated for 8 days, recorded 3 weeks after the end of irradiation. Acquisition time 1.5 min.

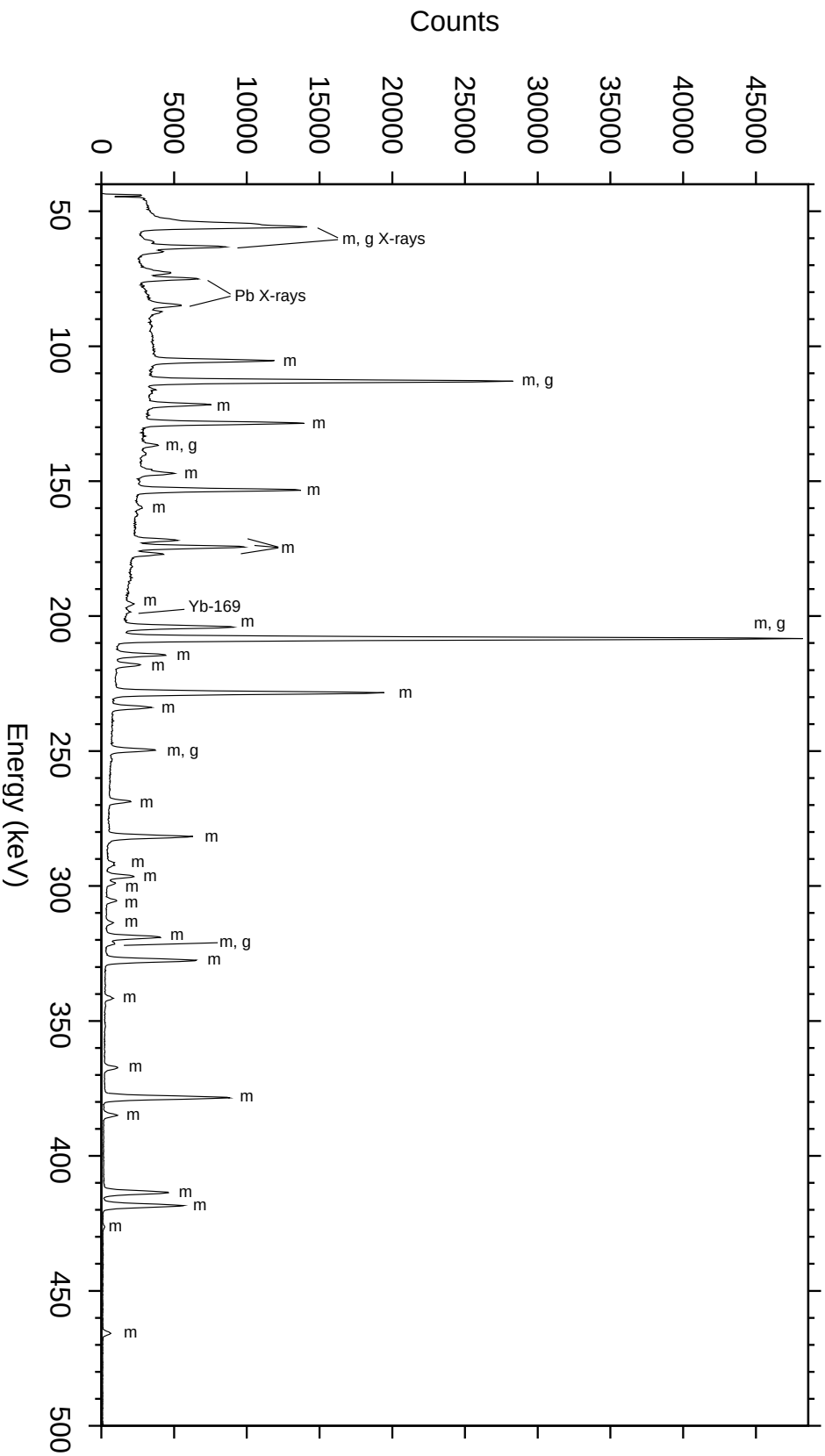

Figure 4.14: First part (40–500 keV) of a γ-ray spectrum of a ^{176}Lu target irradiated for 8 days, recorded 3 months after the end of irradiation. Acquisition time 24 hours. Peaks of ^{177m}Lu are marked by "m", peaks of ^{177}Lu by "g". Except for lutetium isotopes, only ^{169}Yb was observed at 198.0 keV.

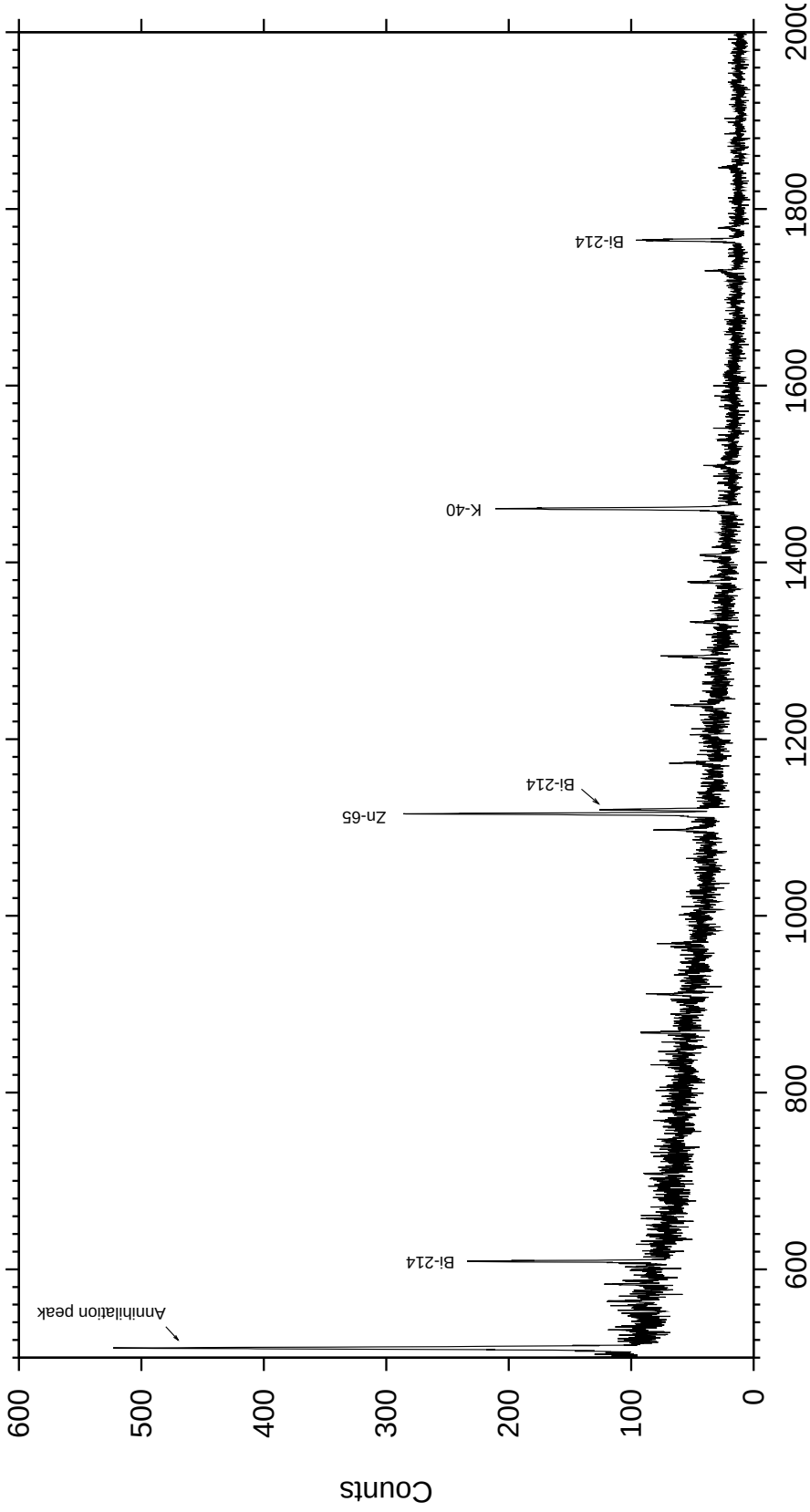

Figure 4.15: Second part (500–2000 keV) of a γ-ray spectrum of a ^{176}Lu target irradiated for 8 days recorded 3 months after the end of irradiation. Acquisition time 24 hours. The isotopes ^{177m}Lu and ^{177}Lu have no peaks in this region. Peaks of ^{65}Zn (activation of Zn impurity in the target) and naturally occuring ^{214}Bi (^{238}U decay chain) and ^{40}K (natural K) were observed.

The 160.5-day isomer ^{177m}Lu, which is inevitably co-produced during the direct route, was experimentally confirmed to be the only relevant long-lived radionuclidic impurity found in ^{177}Lu produced by activation of enriched ^{176}Lu targets. Its experimental content was 0.0068% of ^{177}Lu activity at EOB in the targets irradiated for 8 days in KBA 1-1.

The average ratio of experimental to theoretical ^{177}Lu yield in the indirect production route was found to be 0.91 ± 0.02 for ytterbium targets with 97.1% enrichment (calculated with a cross section of 2.85 b). The effective cross section of the ^{176}Yb (n, γ) ^{177}Yb reaction determined in this work is $\approx$ 2.6 b.

Chapter 5

Conclusion and Outlook

The main goal of the present dissertation was to investigate the feasibility of producing the therapeutic radionuclide ^{177}Lu at the Munich research reactor FRM-II, which was taken in operation in 2004. The radionuclide ^{177}Lu can be produced either directly by the ^{176}Lu$(n,\gamma)^{177}$Lu reaction or indirectly by the ^{176}Yb (n,γ) ^{177}Yb $\xrightarrow{\beta^-}$ ^{177}Lu reaction. Valuable data was acquired on the yield of ^{177}Lu in both production routes and on the content of radionuclidic impurities in the product, including the critical, long-lived $^{177\mathrm{m}}$Lu. In the present work, a reliable method for the calculation of the ^{177}Lu yield was established, which is more accurate than the methods published in the literature. A number of calculations concerning both production routes are presented, which should help to decide which production route is suitable/applicable at the Munich reactor FRM-II. A procedure to recover the produced ^{177}Lu from the direct production reaction in a closed system excluding the introduction of impurities was developed.

Targets of ^{176}Lu$(NO_3)_3$ (direct production route) or ^{176}Yb$(NO_3)_3$ (indirect production route) were irradiated for up to 8 days in KBA 1-1, the capsule irradiation facility providing the highest thermal neutron flux available at FRM-II. The irradiation yield of the direct route was predicted using the Westcott convention, because ^{176}Lu is one of few non-$1/v_n$ nuclides. The neutron flux parameters for the KBA 1-1 irradiation position were determined, a prerequisite for a succesfull application of the Westcott convention. The thermal neutron flux and thermal neutron temperature were monitored during several reactor operation cycles and their average values were

then used for the calculation of the theoretical irradiation yield.

The average ratio of experimental to theoretical ^{177}Lu yields was found to be 1.03 ± 0.03 for lutetium targets with 64.3% enrichment of ^{176}Lu and 1.09 ± 0.04 for lutetium targets with 82.2% enrichment of ^{176}Lu. The effective cross section of the $^{176}\mathrm{Lu}(n,\gamma)^{177}\mathrm{Lu}$ reaction determined in this work is $\approx$ 3700 b for KBA 1-1. According to calculations, the ^{177}Lu irradiation yield shows a maximum at 14.7 days of irradiation in the KBA 1-1. Irradiations longer than 8 days should be carried out in order to find out the exact position of the maximum and to determine the maximum obtainable ^{177}Lu yield. According to calculations, 41.5 µg of ^{176}Lu have to be irradiated for 14.7 days in KBA 1-1 to obtain 1 Ci (37 GBq) of ^{177}Lu.

The irradiation yield of the indirect production route, $^{176}\mathrm{Yb}(n,\gamma)^{177}\mathrm{Yb} \xrightarrow{\beta^-} {}^{177}\mathrm{Lu}$, increases with irradiation time up to the saturation value. The average ratio of experimental and theoretical ^{177}Lu yields was found to be 0.91 ± 0.02 for ytterbium targets with 97.1% enrichment of ^{176}Yb irradiated in KBA 1-1 for up to 8 days (calculated with a cross section of 2.85 b). An effective cross section of 2.6 b, determined in this work, allows an accurate calculation of the irradiation yield of the indirect production route (then A_{exp}/A_{teor} is 0.99 ± 0.02).

The 160.5-day isomer $^{177\mathrm{m}}$Lu, which is inevitably co-produced in the direct route, was experimentally confirmed to be the only relevant long-lived radionuclidic impurity found in ^{177}Lu produced by activation of enriched ^{176}Lu targets. The calculated ratio of $^{177\mathrm{m}}$Lu to ^{177}Lu activities increases with irradiation time, amounting to $<$ 0.01% after 15 days of irradiation in KBA 1-1. The content of $^{177\mathrm{m}}$Lu experimentally found in the targets irradiated for 8 days in KBA 1-1 was 0.0068% at EOB, which agrees well with the values given in the literature.

A system to break the irradiated ampoules and to dissolve the samples was constructed. Up to 98% of the produced ^{177}Lu could be recovered in $<$ 5.5 mL of 0.01 M HCl using this system. Opening the ampoules using this system prevents the contamination of the dissolved sample. The chemical purity of the recovered ^{177}Lu measured by ICP-OES was found to be satisfactory. The total content of transition metals in the ^{177}Lu preparation obtained using the constructed system did not exceed $\sim$1 ppm. The system will allow the integration of remote control or simple robotics, which will be necessary for handling highly active samples.

The maximum obtainable specific activity by the direct production route at FRM-II is 24.5 Ci/mg at the end of a 14.7-day irradiation of a ^{176}Lu target with 83% enrichment of ^{176}Lu. It is reasonable to allow for a three day decay time, mainly due to ^{24}Na produced in the aluminum irradiation capsules. The specific activity will decrease to 18.0 Ci/mg three days after the end of bombardment, which is about the minimum specific activity required by physicians. Irradiating for longer time periods in order to burn-up the target and thus increase the specific activity seems to be not cost-effective. The absolute ^{177}Lu activity decreases while the specific activity increases only slightly (irradiation for 25 days and 3 days of decay provides 19.9 Ci/mg). If a higher specific activity is required, then the indirect production route should be employed.

In spite of providing high specific activity ^{177}Lu free of ^{177m}Lu the indirect production route is ineffective, time consuming, and expensive, when compared with the direct route. Only a very small part of the target is transformed into ^{177}Lu due to the low cross section of ^{176}Yb. The ^{177}Lu recovery from the target requires the employment of an effective Lu/Yb separation method, whose characteristics are crucial for the applicability of this production route. There are only a few laboratories where the indirect route has been employed. One of them is the HFIR at Oak Ridge employing extraction chromatography for a Lu/Yb separation and the other one is the SM reactor at Dimitrovgrad where Yb is reduced and extracted using amalgams ("cementation method"). At both facilities, thermal neutron fluxes of up to 2×10^{15} $cm^{-2}s^{-1}$ are available, so that the mass of the ytterbium target necessary to obtain 1 Ci of ^{177}Lu is only $\sim$3.6–6.5 mg (4–9 days irradiation). Indirect production route is also employed at the NRU reactor at CRL in Canada, where a medium specific activity ^{177}Lu is produced and distributed for customers by MDS Nordion. The development of an efficient and reliable method for the separation of lutetium from ytterbium is required in order to implement the indirect production route at FRM-II. The literature review conducted in the framework of this dissertation resulted in the following ideas, which show possible directions for future research in this area:

- The employment of the cementation method should be considered. If the product purification from traces of mercury can be guaranteed, then it represents one of the best currently available processes for a Lu/Yb separation.

- The feasibility of an electrolytical reduction combined with the precipitation

of ytterbium(II) sulfate or with the extraction of Yb(II)/Lu(III) complexes could be studied. Ytterbium(II) can be stabilized by the use of nonaqueous solvents such as hexamethylphosphoramide (hmpa) or tetrahydrofuran (thf). Chemical reduction of complexes of β-diketonates, e.g. the well known acetylacetonates $Ln(acac)_3$, followed by separation of $Yb(acac)_2$ and $Lu(acac)_3$ using e.g. thin layer chromatography represents also a promising research subject. New complexes of divalent ytterbium have been described recently, such as $[Yb(hmpa)_4(thf)_2]I_2$, $Yb[N(SiMe_3)_2]_2$, $Yb(odpp)_2(thf)_3$ (odpp = 2,6-diphenylphenoxide), which all have the potential to facilitate the Lu/Yb separation [50].

- New systems for the extraction of lanthanide(III) complexes could be developed. Currently, the extraction of lanthanide-polyoxometalate complexes from aqueous solution into chloroform containing amines is studied at MURR (University of Missouri Research Reactor Center), where ^{177}Lu for medical purposes is produced [68].

- One very interesting possibility to separate ^{177}Lu from an ytterbium target is to take advantage of the Szilard-Chalmers effect. If ytterbium can be incorporated into a radiation-stable compound and then irradiated in a reactor, ^{177}Lu can be released from that compound as a result of the ^{177}Yb decay accompanied by energy release causing a break of the chemical bonds holding the original ^{176}Yb. The target compound could e.g. be prepared by ytterbium stearate pyrolysis resulting in insoluble YbC_x with low atomic density allowing the release of ^{177}Lu from the compound. During the irradiation, the released ^{177}Lu should be stabilized in a new compound to prevent its reincorporation into the original compound. Ideally, the solid YbC_x should be continuously washed with solution containing an agent forming a lutetium complex during the irradiation.

Bibliography

[1] F. Rösch (volume editor), A. Vértes, S. Nagy, and Z. Klencsár (series editors). *Handbook of Nuclear Chemistry: Radiochemistry and Radiopharmaceutical Chemistry in Life Sciences*, volume 4. Kluwer Academic Publishers, Amsterdam, 2003.

[2] Massachusetts institute of technology. The basics of boron neutron capture therapy. http://web.mit.edu/nrl/www/bnct/info/description/description.html, accessed July 11, 2007.

[3] The National Association for Proton Therapy. http://www.proton-therapy.org/, accessed July 11, 2007.

[4] E. Haettner, H. Iwase, and D. Schardt. Experimental fragmentation studies with ^{12}C therapy beams. *Radiation Protection Dosimetry*, 122:485–487, 2006.

[5] W. A. Volkert and T. J. Hoffman. Therapeutic radiopharmaceuticals. *Chemical Reviews*, pages 2269–2292, 1999.

[6] H. L. Atkins. Overview of nuclides for bone pain palliation. *Applied radiation and isotopes*, 49:277–283, 1998.

[7] A. M. Evens and L. I. Gordon. Radioimmunotherapy in non-Hodgkin's lymphoma: trials of yttrium 90-labeled ibritumomab tiuxetan and beyond. *Clinical Lymphoma*, 5 Suppl 1:S11–15, 2004.

[8] W. J. Taylor, M. M. Corkill, and C. N. Rajapaske. A retrospective review of yttrium-90 synovectomy in the treatment of knee arthritis. *Rheumatology*, 36:1100–1105, 1997.

[9] R. Jacob, T. Smith, B. Prakasha, and T. Joannides. Yttrium-90 synovectomy in the management of chronic knee arthritis: a single institution experience. *Rheumatology International*, 23:216–220, 2003.

[10] L. Mausner and S. Srivastava. Selection of radionuclides for radioimmunotherapy. *Medical Physics*, 20:503–509, 1993.

[11] M. Neves, A. Kling, and A. Oliveira. Radionuclides used for therapy and suggestion for new candidates. *Journal of Radioanalytical and Nuclear Chemistry*, 266:377–384, 2005.

[12] J. J. M. De Goeij and M. L. Bonardi. How do we define the concepts specific activity, radioactive concentration, carrier, carrier-free and no-carrier-added? *Journal of Radioanalytical and Nuclear Chemistry*, 263:13–18, 2005.

[13] W. A. P. Breeman, M. De Jong, T. J. Visser, J. L. Erion, and E. P. Krenning. Optimising conditions for radiolabelling of DOTA-peptides with ^{90}Y, ^{111}In and ^{177}Lu at high specific activities. *European Journal of Nuclear Medicine and Molecular Imaging*, 30:917–920, 2003.

[14] S. M. Qaim. Therapeutic radionuclides and nuclear data. *Radiochimica Acta*, 89:297–302, 2001.

[15] National nuclear data center. Brookhaven national laboratory. http://www.nndc.bnl.gov/nudat2/, accessed May 21, 2007.

[16] S. Vallabhajosula, I. I. Kuji, K. A. Hamacher, S. Konishi, L. Kostakoglu, P. A. Kothari, M. I. Milowski, D. M. Nanus, N. H. Bander, and S. J. Goldsmith. Pharmacokinetics and Biodistribution of ^{111}In- and ^{177}Lu-Labeled J591 Antibody Specific for Prostate-Specific Membrane Antigen: Prediction of ^{90}Y-J591 Radiation Dosimetry Based on ^{111}In or ^{177}Lu? *The Journal of Nuclear Medicine*, 46:634–641, 2005.

[17] W. H. Bakker, W. A. P. Breeman, D. J. Kwekkeboom, L. C. De Jong, and E. P. Krenning. Practical aspects of peptide receptor radionuclide therapy with [^{177}Lu][DOTA^{0}, Tyr^{3}]octreotate. *The Quarterly Journal of Nuclear Medicine and Molecular Imaging*, 50:265–271, 2006.

[18] A. Schmitt, P. Bernhardt, O. Nilsson, H. Ahlman, L. Kolby, H. R. Maecke, and E. Forssell-Aronsson. Radiation therapy of small cell lung cancer with ^{177}Lu-DOTA-Tyr^3-octreotate in an animal model. *Journal of Nuclear Medicine*, 45(9):1542–1548, 2004.

[19] J. J. M. Teunissen, D. J. Kwekkeboom, and E. P. Krenning. Quality of life in patients with gastroenteropancreatic tumors treated with [^{177}Lu-DOTA^0, Tyr^3]octreotate. *Journal of Clinical Oncology*, 13:2724–2729, 2004.

[20] F. Forrer, H. Uusijarvi, D. Storch, H. R. Maecke, and J. Mueller-Brand. Treatment with ^{177}Lu-DOTATOC of Patients with Relapse of Neuroendocrine Tumors After Treatment with ^{90}Y-DOTATOC. *Journal of Nuclear Medicine*, 46(8):1310–1316, 2005.

[21] C. J. Smith, H. Gali, G. L. Sieckman, D. L. Hayes, N. K. Owen, D. G. Mazuru, W. A. Volkert, and T. J. Hoffman. Radiochemical investigations of ^{177}Lu-DOTA-8-Aoc-BBN[7-14]NH_2: an in vitro/in vivo assessment of the targeting ability of this new radiopharmaceutical for PC-3 human prostate cancer cells. *Nuclear Medicine and Biology*, 30:101–109, 2003.

[22] L. E. Lantry, E. Cappelletti, M. E. Maddalena, J. S. Fox, W. Feng, J. Chen, R. Thomas, S. M. Eaton, N. J. Bogdan, T. Arunachalam, J. C. Reubi, N. Raju, E. C. Metcalfe, L. Lattuada, K. E. Linder, R. E. Swenson, M. F. Tweedle, and A. D. Nunn. ^{177}Lu-AMBA: Synthesis and Characterization of a Selective ^{177}Lu-Labeled GRP-R Agonist for Systemic Radiotherapy of Prostate Cancer. *The Journal of Nuclear Medicine*, 47:1144–1152, 2006.

[23] S. Panigone and A. D. Nunn. Lutetium-177-labeled gastrin releasing peptide receptor binding analogs: a novel approach to radionuclide therapy. *The Quarterly Journal of Nuclear Medicine and Molecular Imaging*, 50:310–321, 2006.

[24] R. Markwalder and J. C. Reubi. Gastrin-releasing peptide receptors in the human prostate: Relation to neoplastic transformation. *Cancer Research*, 59(5):1152–1159, 1999.

[25] M. Gugger and J. C. Reubi. Gastrin-releasing peptide receptors in non-neoplastic and neoplastic human breast. *The American Journal of Pathology*, 155(6):2067–2076, 1999.

[26] J. C. Reubi. Peptide receptors as molecular targets for cancer diagnosis and therapy endocr. rev. 24: 389-427,. *Endocrine Reviews*, 24:389–427, 2003.

[27] J. Magill, G. Pfennig, and J. Galy. Karlsruher Nuklidkarte, 7th edition. European Communities, 2006.

[28] S. F. Mughabghab. *Atlas of Neutron Resonances, Resonance Parameters and Thermal Cross Sections, Z=1-100.* Elsevier, 2006.

[29] V. S. Shirley. Nuclear data sheets for A = 169. *Nuclear Data Sheets*, 64:505–636, 1991.

[30] E. Browne and H. Junde. Nuclear Data Sheets for A = 176. *Nuclear Data Sheets*, 84:337–486, 1998.

[31] F. G. Kondev. Nuclear Data Sheets for A = 177. *Nuclear Data Sheets*, 98:801–1095, 2003.

[32] M. S. Basunia. Nuclear Data Sheets for A = 175. *Nuclear Data Sheets*, 102:719–900, 2004.

[33] J. Kopecky. Atlas of Neutron Capture Cross Sections (IAEA). http://www-nds.iaea.org/ngatlas2/, accessed March 30, 2007.

[34] P. S. Balasubramanian. Separation of carrier-free lutetium-177 from neutron irradiated natural ytterbium target. *Journal of Radioanalytical and Nuclear Chemistry*, 185:305–310, 1994.

[35] N. A. Lebedev and A. F. Novgorodov and R. Misiak and J. Brockmann and F. Rösch. Radiochemical separation of no-carrier-added ^{177}Lu as produced via the ^{176}Yb(n,γ)^{177}Yb $\rightarrow$ ^{177}Lu process. *Applied Radiation and Isotopes*, 53:421–425, 2000.

[36] K. Hashimoto, H. Matsuoka, and S. Uchida. Production of no-carrier-added ^{177}Lu via the ^{176}Yb(n,γ)^{177}Yb $\rightarrow$ ^{177}Lu process. *Journal of Radioanalytical and Nuclear Chemistry*, 255:575–579, 2003.

[37] S. Mirzadeh et al. Method for preparing high specific activity ^{177}Lu. U.S. Patent 6,716,353 B1, April 6 2004.

[38] E. P. Horwitz, D. R. McAlister, A. H. Bond, R. E. Barrans, and J. M. Williamson. A process for the separation of ^{177}Lu from neutron irradiated ^{176}Yb targets. *Applied Radiation and Isotopes*, 63:23–36, 2005.

[39] F. F. Knapp, K. R. Ambrose, A. L. Beets, H. Luo, D. W. McPherson, and S. Mirzadeh. Nuclear medicine program progress report for quarter ending September 30, 1995. Technical Report ORNL/TM–13107, Oak Ridge National Laboratory, 1995.

[40] F. F. Knapp, S. Mirzadeh, A. L. Beets, M. Du, J. A. Klein, and M. Garland. "Direct" production of lutetium-177 (Lu-177) from enriched Lu-176 in a high flux reactor - the only practical route to provide high multi curie levels of high specific activity Lu-177 required for routine clinical use. In C. Chemaly, B. J. Allen, and H. Bonet, editors, *Proceedings of the 5th International Conference on Isotopes (5ICI), 25-29 April 2005, Brussels, Belgium*, 2005.

[41] Y. G. Toporov, V. A. Tarasov, O. I. Andreev, E. A. Zotov, V. N. Kupriyanov, V. D. Gavrilov, and A. L. Semenov. Production of the ^{177}Lu preparation of high specific activity in the SM research reactor. In C. Chemaly, B. J. Allen, and H. Bonet, editors, *Proceedings of the 5th International Conference on Isotopes (5ICI), 25-29 April 2005, Brussels, Belgium*, 2005.

[42] R. Mikolajczak, J. L. Parus, D. Pawlak, E. Zakrzewska, W. Michalak, and I. Sasinowska. Reactor produced ^{177}Lu of specific activity and purity suitable for medical applications. *Journal of Radioanalytical and Nuclear Chemistry*, 257:53–57, 2003.

[43] D. Pawlak, J. L. Parus, I. Sasinowska, and R. Mikolajczak. Determination of elemental and radionuclidic impurities in ^{177}Lu used for labeling of radiopharmaceuticals. *Journal of Radioanalytical and Nuclear Chemistry*, 261:469–472, 2004.

[44] R. Mikolajczak, D. Pawlak, and J. L. Parus. Separation of microgram quantities of ^{177}Lu from milligram amounts of Yb by the extraction chromatography. In C. Chemaly, B. J. Allen, and H. Bonet, editors, *Proceedings of the 5th International Conference on Isotopes (5ICI), 25-29 April 2005, Brussels, Belgium*, 2005.

[45] M. R. A. Pillai, S. Chakraborty, T. Das, M. Venkatesh, and N. Ramamoorthy. Production logistics of ^{177}Lu for radionuclide therapy. *Applied Radiation and Isotopes*, 59:109–118, 2003.

[46] T. Das, S. Chakraborty, S. Banerjee, and M. Venkatesh. On the preparation of a therapeutic dose of ^{177}Lu-labeled DOTA-TATE using indigenously produced ^{177}Lu in medium flux reactor. *Applied Radiation and Isotopes*, 65:301–308, 2007.

[47] MDS Nordion. http://www.nordion.com/products/medical-isotopes-lutetium-177.htm, accessed July 17, 2007.

[48] A. Hermanne, E. Lavie, M. Goldberg, and S. Takacs. Deuteron-induced reactions of Yb: a carrier-free alternative to reactor-produced ^{177}Lu? In C. Chemaly, B. J. Allen, and H. Bonet, editors, *Proceedings of the 5th International Conference on Isotopes (5ICI), 25-29 April 2005, Brussels, Belgium*, 2005.

[49] J. H. Forsberg, Y. Marcus, and T. Moeller. *Gmelin Handbook of Inorganic Chemistry: Sc, Y, La-Lu Rare Earth Elements*. Number Part D6. Springer-Verlag, Berlin, 1983.

[50] S. Cotton. *Lanthanide and Actinide Chemistry*. John Wiley & Sons, 2006.

[51] G. R. Choppin and R. J. Silva. Separation of the lanthanides by ion exchange with alpha-hydroxyisobutyric acid. *Journal of Inorganic and Nuclear Chemistry*, 3:153–154, 1956.

[52] M. Marhol. *Ion Exchangers in Analytical Chemistry: Their Properties and Use in Inorganic Chemistry*. Academia, Prague, 1982.

[53] F. O. Denzler and N. A. Lebedev, A. F. Novgorodov, F. Rösch and S. M. Qaim. Production and radiochemical separation of ^{147}Gd. *Applied Radiation and Isotopes*, 48:319–326, 1997.

[54] S. Lahiri, K. J. Volkers, and B. Wierczinski. Production of ^{166}Ho through $^{164}\mathrm{Dy}(n,\gamma)^{165}\mathrm{Dy}(n,\gamma)^{166}\mathrm{Dy}(\beta^-)^{166}$Ho and separation of ^{166}Ho. *Applied Radiation and Isotopes*, 61:1157–1161, 2004.

[55] E. P. Horwitz and C. A. A. Bloomquist. Chemical separations for super-heavy element searches in irradiated uranium targets. *Journal of Inorganic and Nuclear Chemistry*, 37:425–434, 1975.

[56] E. P. Horwitz, C. A. A. Bloomquist W. H. Delphin, and G. F. Vandegrift. Radiochemical and Isotope Separations by High-Efficiency Liquid-Liquid Chromatography. *Journal of Chromatography*, 125:203–218, 1976.

[57] Eichrom Technologies, Inc. http://eichrom.com/index.cfm, accessed April 16, 2007.

[58] F. F. (Russ) Knapp, S. Mirzadeh, A. L. Beets, and M. Du. Production of therapeutic radioisotopes in the ORNL High Flux Isotope Reactor (HFIR) for applications in nuclear medicine, oncology and interventional cardiology. *Journal of Radioanalytical and Nuclear Chemistry*, 263:503–509, 2005.

[59] J. K. Marsh. Rare-earth metal amalgams. Part I. The reaction between sodium amalgam and rare-earth acetate and chloride solutions. *Journal of the Chemical Society*, pages 398–401, 1942.

[60] J. K. Marsh. Rare-earth metal amalgams. Part II. The separation of neodymium, samarim, and gadolinium. *Journal of the Chemical Society*, pages 523–526, 1942.

[61] J. K. Marsh. Rare-earth metal amalgams. Part IV. The isolation of europium. *Journal of the Chemical Society*, pages 531–533, 1943.

[62] J. K. Marsh. Rare-earth metal amalgams. Part III. The separation of ytterbium from its neighbours. *Journal of the Chemical Society*, 2:8–10, 1943.

[63] M. F. Barrett, D. Sweasey, and N. E. Topp. The extraction of lanthanons with alkali metal amalgams–I : Samarium and ytterbium. *Journal of Inorganic and Nuclear Chemistry*, 24:571–586, 1962.

[64] F. R. Lawless and M. A. Wahlgren. A rapid carrier-free separation method for divalent rare earths. *Journal of Radioanalytical and Nuclear Chemistry*, 5:11–20, 1970.

[65] A. F. Novgorodov, V. A. Khalkin, and P'en Wang Ch'uang. Cementation of microamounts of carrier free radioactive isotopes of rare-earth elemens from acetate solutions by sodium amalgam. *Radiokhimiya (English translation)*, 8:347–352, 1966.

[66] M. Schädel, T. Trautmann, and G. Hermann. Fast separation of lanthanides by high pressure liquid chromatography. *Radiochimica Acta*, 24:27–31, 1977.

[67] Bio-Rad Laboratories. Aminex ion exchange resins, instruction manual. http://www.bio-rad.com/LifeScience/pdf/Bulletin_9132.pdf, accessed April 23, 2007.

[68] L. Francesconi, R. Howell, I. R. Jones, and C. S. Cutler. Evaluation of polyoxometalates to extract lanthanides. *Journal of Labelled Compounds and Radiopharmaceuticals*, 48(S1):S106–S115, 2005.

[69] International atomic energy agency. *Manual for reactor produced radioisotopes*, 2003. IAEA-TECDOC-1340.

[70] Neutron fluence measurements. Technical Report Series No. 107, International atomic energy agency, 1970.

[71] X. Lin, R. Henkelmann, A. Türler, H. Gerstenberg, and F. De Corte. Neutron flux parameters at irradiation positions in the new research reactor FRM-II. *Nuclear Instruments and Methods in Physics Research Section A: Accelerators, Spectrometers, Detectors and Associated Equipment*, 564:641–644, 2006.

[72] O. T. Høgdahl. Neutron absorption in pile neutron activation analysis. Michigan Memorial Phoenix Project MMPP-226-1, University of Michigan, Ann Arbor, 1962.

[73] O. T. Høgdahl. In *Proceedings of IAEA Symposium on Radiochemical Methods of Analysis*, volume 1, page 23. IAEA, 1965.

[74] S. Jovanovic, P. Vukotic, B. Smodis, R. Jacimovic, N. Mihaljevic, and P. Stegnar. Epithermal neutron flux characterization of the TRIGA MARK II reactor, Ljubljana, Yugoslavia, for use in NAA. *Journal of Radioanalytical and Nuclear Chemistry*, 129:343 – 349, 1989.

[75] F. De Corte, A. Simonits, F. Bellemans, M. C. Freitas, S. Jovanović, B. Smodiš, G. Erdtmann, H. Petri, and A. De Wispelaere. Recent advances in the k_0-standardization of neutron activation analysis: Extensions, applications, prospects. *Journal of Radioanalytical and Nuclear Chemistry*, 169:125–158, 1993.

[76] C. H. Westcott. The specification of neutron flux and nuclear cross-sections in reactor calculations. *Journal of Nuclear Energy*, 2:59–75, 1955.

[77] F. De Corte, F. Bellemans, P. De Neve, and A. Simonits. The use of a modified Westcott-formalism in the k_0-standardization of NAA: The state of affairs. *Journal of Radioanalytical and Nuclear Chemistry*, 179:93–103, 1994.

[78] F. De Corte and A. Simonits. Recommended nuclear data for use in the k_0 standardization of neutron activation analysis. *Atomic Data and Nuclear Data Tables*, 85:47–67, 2003.

[79] K. H. Lieser. *Nuclear and Radiochemistry: Fundamentals and Applications.* Wiley-WCH, 2^{nd} edition, 2001.

[80] X. Lin, F. Baumgärtner, and X. Li. The program "MULTINAA" for various standardization methods in neutron activation analysis. *Journal of Radioanalytical and Nuclear Chemistry*, 215(2):179–191, 1997.

[81] N. E. Holden. Temperature Dependence of the Westcott g-factor for Neutron Reactions in Activation Analysis. (Technical Report). *Pure and Applied Chemistry*, 71:2309–2315, 1999.

[82] R. B. Firestone. *Table of isotopes.* Ed. Virginia S. Shirley, 8th edition, 1996.

[83] Handbook on nuclear activation data. Technical Report series No. 273, International atomic energy agency, 1987.

[84] W. Bakker (Erasmus Medical Center Netherlands). Personal communication.